GAIN OF THE MAGNETIC AMPLIFIER

THUC, DO KIM

GAIN OF THE MAGNETIC AMPLIFIER

*****

Do Kim-Thuc

GAIN OF THE MAGNETIC AMPLIFIER

By

Do Kim-Thuc

Lieutenant, Vietnam Navy

Submitted in partial fulfillment of
the requirement for the degree of

MASTER OF SCIENCE
IN
ELECTRICAL ENGINEERING

United States Naval Postgraduate School
Monterey, California

1 9 6 2

GAIN OF THE MAGNETIC AMPLIFIER

By

Do Kim-Thuc

This work is accepted as fulfilling

the thesis requirements for the degree of

MASTER OF SCIENCE

IN

ELECTRICAL ENGINEERING

from the

United States Naval Postgraduate School

ABSTRACT

In this thesis, the gain of the magnetic amplifier is derived theoretically as a function of different parameters of the circuit. An experimental circuit of a series-connected magnetic amplifier with a resistive load is set up to verify the theoretical results.

Starting from Kirchoff's Voltage Law and Ampere's Law applied to the circuit, with the polynomial representation of the magnetization curve of the core material, a set of equations for currents and fluxes is obtained. These equations contain nonlinear terms. The Poisson perturbation method is used to solve the simultaneous nonlinear equations of fluxes.

Successive approximations of core fluxes and currents can be made to get the theoretical results as close as required to the experimental results. Only the first approximation is computed in this thesis.

The only difficulty one can encounter when using the perturbation method is the lack of knowledge of the region of convergence. The smallness of the coefficients which are negative of the nonlinear factors in this particular application contributes to the rapid diminution of the contribution from successive approximations.

ACKNOWLEDGEMENTS

The author would like to express his appreciation to Dr. Charles H. Rothauge for his advice and encouragement, to Dr. J. B. O'Toole for his assistance in the solving of some mathematical equations and to Professor R. B. Yarbrough for his helpful advice and instruction in the use of the instruments of measurement.

TABLE OF CONTENTS

LIST OF ILLUSTRATIONS

TABLE OF SYMBOLS AND ABBREVIATIONS

Symbol	Description	Unit
e_1	signal voltage	volt
e_2	carrier voltage	volt
e_o	output voltage	volt
E_{1m}	maximum amplitude of signal voltage	volt
E_{2m}	maximum amplitude of carrier voltage	volt
E_b	bias voltage	volt
f_1 and f_2	nonlinear factors in magnetic amplifier	volt/turn
$f\phi_x$	partial derivative of f with respect to ϕ_x	
$f\phi_y$	partial derivative of f with respect to ϕ_y	
F_a	magnetomotive force of core a	ampere-turn
F_b	magnetomotive force of core b	ampere-turn
i_1	input-circuit current	ampere
i_2	output-circuit current	ampere
k_n	constants for magnetic amplifier	ampere-turn/weber
K	voltage gain	dimensionless
$2L_{10}$	linearized inductance of input-circuit	henry
$2L_{20}$	linearized inductance of output-circuit	henry
N_1	number of turns of input-circuit winding	turn
N_2	number of turns of output-circuit winding	turn
$2R_1$	control circuit resistance	ohm

[illegible]

[illegible]	[illegible]	[illegible]
[illegible]	[illegible]	[illegible]
[illegible]	[illegible]	[illegible]
[illegible]	[illegible]	[illegible]
[illegible]	[illegible]	[illegible]
[illegible]	[illegible]	[illegible]
[illegible]	[illegible]	[illegible]
[illegible]	[illegible]	[illegible]
[illegible]	[illegible]	[illegible]
[illegible]	[illegible]	[illegible]
[illegible]	[illegible]	[illegible]
[illegible]	[illegible]	[illegible]
[illegible]	[illegible]	[illegible]
[illegible]	[illegible]	[illegible]
[illegible]	[illegible]	[illegible]
[illegible]	[illegible]	[illegible]
[illegible]	[illegible]	[illegible]
[illegible]	[illegible]	[illegible]
[illegible]	[illegible]	[illegible]
[illegible]	[illegible]	[illegible]

Symbol	Description	Unit
$2R_2$	output circuit resistance	ohm
R_L	load resistance	ohm
t	time	second
T_1	delay time of control circuit in linear approximation	second
T_2	delay time of output circuit in linear approximation	second
α	constant	dimensionless
β	constant	dimensionless
ρ_1 and ρ_2	coefficients of nonlinear factors	dimensionless
ϕ_a	total flux in core a	weber
ϕ_b	total flux in core b	weber
ω	angular velocity of carrier frequency	radian/second
Ω	angular velocity of signal frequency	radian/second

I-Introduction-

In most analyses of magnetic amplifiers, the steady state and transient responses are obtained by piecewise linear methods or by the assumption of a direct current component and a sine wave of carrier frequency.

The basis of operation of the magnetic amplifier depends on the nonlinear characteristics of the core material. This nonlinearity makes the mathematical analysis tedious.

This thesis presents a quantitative analysis of the sinusoidal response of a series connected magnetic amplifier expressed in dimensionless form.

The method used to solve the nonlinear system equations is Poisson's method. Kirchhoff's voltage law and Ampere's line integral law are applied to the circuit to set up its fundamental equations. The magnetization curve of the core material is represented by a general polynomial. The problem is then reduced to solving the simultaneous nonlinear equations of the fluxes in both cores. From that, successive approximations of core fluxes and currents can be obtained. But only the first approximation has been done in this thesis.

The purpose of this paper is to treat the general problem of the gain in magnetic amplifiers. A general type series connected magnetic amplifier shown in Fig. 1 is chosen for study. A biased sinusoidal voltage is used as input; and a power supply of higher frequency, as carrier. The output is therefore a modulated signal subjected to harmonic distortions of both signal and carrier frequencies. The waveform of the envelope of the modulated output, i.e. the fundamental component and

harmonic contents of signal frequency has been analyzed. The following results have been obtained in dimensionless form and checked by experiment:

a) General solutions for fluxes and currents

b) Magnitude and phase angle of fundamental gain as a function of the system parameters

c) Harmonic distortions of the response

Poisson's method is most valuable in cases where Poisson's series for the flux converges rapidly, and the core material used has a gradually varying incremental permeability. The problem of d.c. controlled magnetic amplifier can be analyzed by this method by considering it as a special case of the present general analysis.

The present analysis has the following limitations:

I-If Poisson's series converges slowly, the work will be very laborious.

II-If Poisson's series diverges, this method will no longer be valid.

III-The core material should have a gradually varying incremental permeability such that it can be suitably represented by a polynomial of few terms.

II-Theoretical Analysis -

1. Assumptions.

The magnetic amplifier circuit used in this analysis is that of a series-connected magnetic amplifier shown in Fig. 1 with a resistance load. The following assumptions are made:

a) Both cores have the same electrical and magnetic properties,

b) Effects due to eddy-current and hysteresis losses in the core are neglected,

c) The magnetization characteristics can be suitably represented by a polynomial

2. Fundamental equations.

Applying Kirchhoff's voltage law to the circuit in Fig. 2

$$E_{1m} \sin \omega t + E_b = 2R_1 i_1 + N_1 \frac{d\phi_a}{dt} + N_1 \frac{d\phi_b}{dt} \qquad (1)$$

$$E_{2m} \sin \omega t = (2R_2 + R_L) i_2 + N_2 \frac{d\phi_a}{dt} - N_2 \frac{d\phi_b}{dt} \qquad (2)$$

Applying Ampere's Law to the magnetic circuits of the cores (core a and core b) (Fig. 2).

$$F_a = N_1 i_1 + N_2 i_2 \qquad (3)$$

$$F_b = N_1 i_1 - N_2 i_2 \qquad (4)$$

The magnetization characteristics of the magnetic saturable reactors is represented by a polynomial containing a sufficient number of terms to secure the exactness of fit. In general:

$$F_a = \sum_n k_n \phi_a^n \qquad (5)$$

$$F_b = \sum_n k_n \phi_b^n \qquad (6)$$

where n's are odd integers only, due to the skew-symmetry of the magnetization characteristics.

The 6 above equations constitute the fundamental system equations of the magnetic amplifier circuit shown in Fig. 1. These will be solved to determine the transient andsteady state of currents i_1 and i_2.

Substituting equations (5) and (6) into equations (3) and (4) respectively, then solving for i_1 and i_2, in terms of ϕ

$$i_1 = \frac{1}{2N_1}\left[\sum_n k_n \phi_a^n + \sum_n k_n \phi_b^n\right] \qquad (7)$$

$$i_2 = \frac{1}{2N_2}\left[\sum_n k_n \phi_a^n - \sum_n k_n \phi_b^n\right] \qquad (8)$$

Combining corresponding terms of the polynomials in the above equations,

$$i_1 = \frac{1}{2N_1} \sum_n k_n \left(\phi_a^n + \phi_b^n\right) \qquad (9)$$

$$i_2 = \frac{1}{2N_2} \sum_n k_n \left(\phi_a^n - \phi_b^n\right) \qquad (10)$$

Substituting equation(9) into equation (1) and equation (10) into equation (2),

$$E_{1m} \sin \Omega t + E_b = \frac{R_1}{N_1} \sum_n k_n \left(\phi_a^n + \phi_b^n\right) + N_1 \frac{d}{dt}\left(\phi_a + \phi_b\right) \qquad (11)$$

$$E_{2m} \sin \omega t = \frac{2R_2 + R_L}{2N_2} \sum_n k_n \left(\phi_a^n - \phi_b^n\right) + N_2 \frac{d}{dt}\left(\phi_a - \phi_b\right) \qquad (12)$$

Let

$$\phi_a + \phi_b = 2\phi_x \qquad (13)$$

$$\phi_a - \phi_b = 2\phi_y \qquad (14)$$

we may then write,

$$\sum_n k_n \left(\phi_a^n + \phi_b^n\right) = 2k_1 \phi_x + \sum_j k_j \left[\left(\phi_x + \phi_y\right)^j + \left(\phi_x - \phi_y\right)^j\right] \qquad (15)$$

$$\sum_n k_n \left(\phi_a^n - \phi_b^n\right) = 2k_1 \phi_y + \sum_j k_j \left[\left(\phi_x + \phi_y\right)^j - \left(\phi_x - \phi_y\right)^j\right] \qquad (16)$$

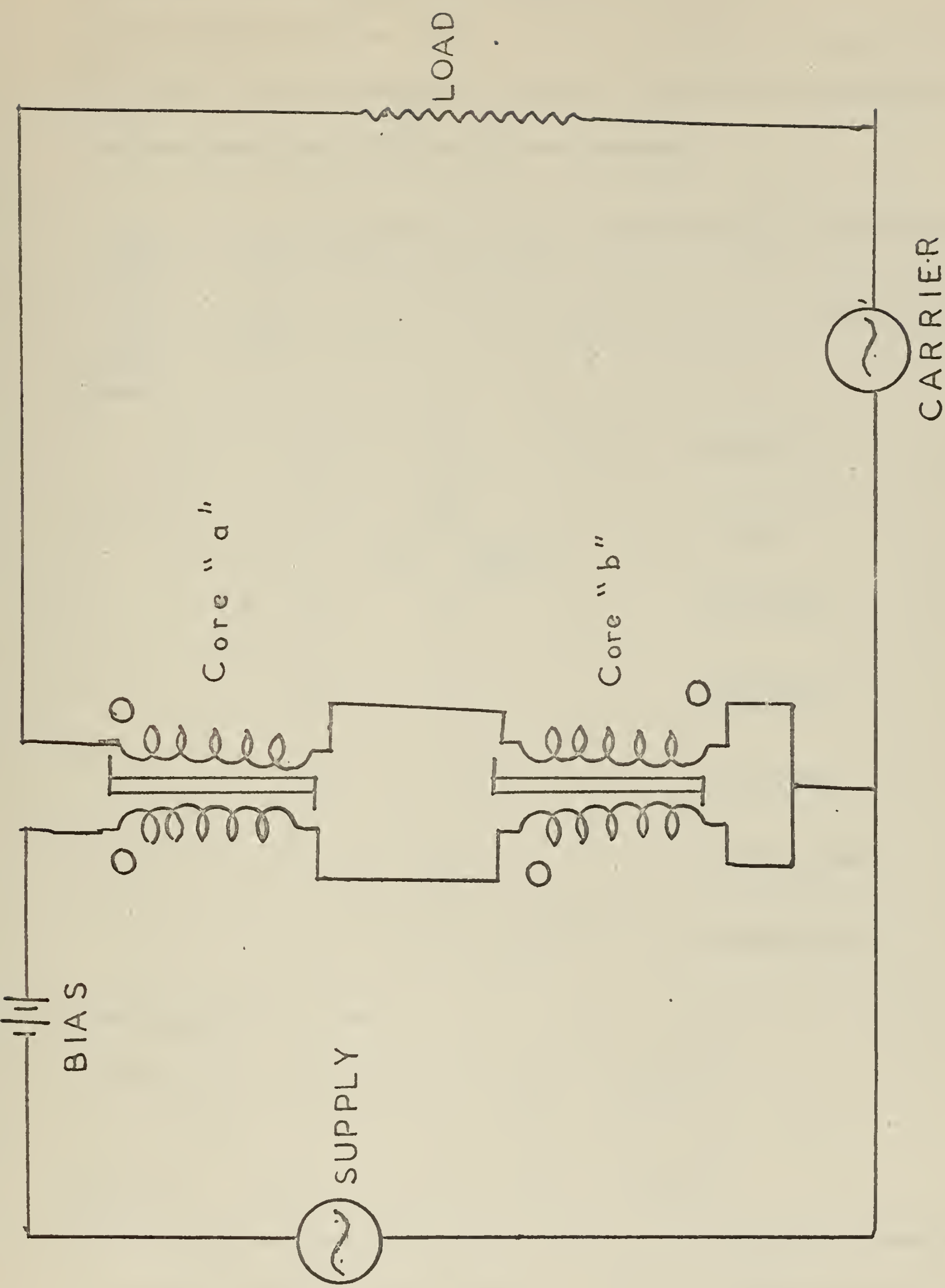

FIG. 1 - SERIES - CONNECTED MAGNETIC AMPLIFIER

where the j's are odd integers greater than unity.

Substituting equations (13), (14), (15) and (16) into equations (11) and (12), then rearranging the results, the following **nonlinear**, simultaneous equations for ϕ_x and ϕ_y are obtained:

$$\frac{d\phi_x}{dt} = \left(-\frac{1}{T_1}\phi_x + V_{1m}\cos\Omega t + V_b\right) + \rho_1 f_1(\phi_x, \phi_y) \qquad \text{volt/turn} \quad (17)$$

$$\frac{d\phi_y}{dt} = \left(-\frac{1}{T_2}\phi_y + V_{2m}\cos\Omega t\right) + \rho_2 f_2(\phi_x, \phi_y) \qquad \text{volt/turn} \quad (18)$$

where

$$T_1 = \frac{N_1^2}{r_1 R_1} \qquad \text{second} \quad (19)$$

$$T_2 = \frac{N_2^2}{r_2\left(1 + \frac{R_1}{2R_2}\right)R_1} \qquad \text{second} \quad (20)$$

$$V_{1m} = \frac{E_{1m}}{[illegible]} \qquad \text{volt/turn} \quad (21)$$

$$V_{[illegible]} = [illegible] \qquad \text{volt/turn} \quad (22)$$

$$V_b = [illegible] \qquad \text{volt/turn} \quad (23)$$

$$\rho_1 = -\frac{R_1}{[illegible]}\sigma \qquad \text{dimensionless} \quad (24)$$

$$\rho_2 = -\frac{R_2\left(1 + [illegible]\right)\sigma}{[illegible]} \qquad \text{dimensionless} \quad (25)$$

Rearranging the terms,

$$f_1(\phi_x, \phi_y) = \frac{1}{\sigma}\sum_j b_j\left[(\phi_x + \phi_y)^j + (\phi_x - \phi_y)^j\right] \quad (26)$$

$$f_2(\phi_x, \phi_y) = \frac{1}{\sigma}\sum_j b_j\left[(\phi_x + \phi_y)^j - (\phi_x - \phi_y)^j\right] \quad (27)$$

where σ is a dimensional factor which is introduced in these equations in order to make the coefficients and dimensionless. Numerically $\sigma = 1$ and has dimensions of turns^2/ohm. By examining equations (13) and (14) and the circuit diagram in Fig. 2, it is found that ϕ_x is the flux principally produced by the control current and ϕ_y is the flux

produced by the output current.

In equation (18):

$$\frac{d\phi_y}{dt} = \text{[illegible]} \qquad \text{volt/turn} \qquad (18)$$

The left hand side term is the generated counter emf along the output circuit, and the first term of the righthand side is the linear part of the voltage drop of the fundamental component of the carrier frequency; the second term is the applied carrier voltage and the last term is the voltage drops of all harmonics.

Equation (17) has a corresponding physical meaning for the input circuit.

From equations (13) and (14),

$$\phi_a = \phi_x + \phi_y \qquad \text{weber} \qquad (28)$$

$$\phi_b = \phi_x - \phi_y \qquad \text{weber} \qquad (29)$$

Substituting equations (29) and (30) into equations (9) and (10), the solutions of the current responses in terms of ϕ_x and ϕ_y are obtained:

$$i_1 = \text{[illegible]} \qquad (30)$$

$$i_2 = \text{[illegible]} \qquad (31)$$

If the order of the polynomial in the above equations is allowed to increase indefinitely, equations (30) and (31) become infinite series. The convergence of this infinite series is proved in Appendix A.

Equations (30) and (31) for the current responses can be utilized only if simultaneous nonlinear equations (17) and (18) can be solved for ϕ_x and ϕ_y. In these nonlinear equations, [illegible], the coefficient of the nonlinear factor f_1, and [illegible], the coefficient of the nonlinear factor f_2 are much less than unity by virtue of the low internal resistances of

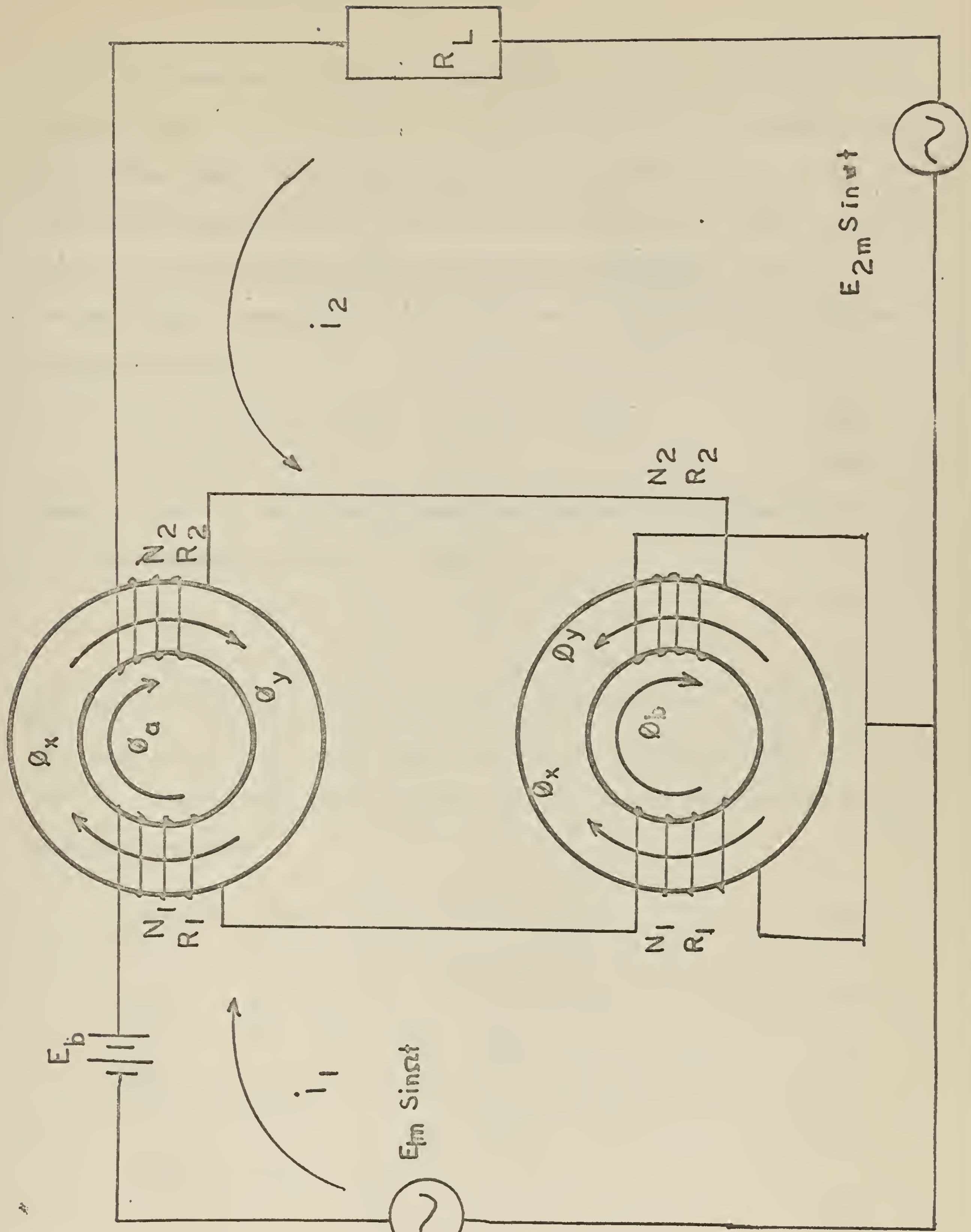

FIG. 2 - SERIES-CONNECTED MAGNETIC AMPLIFIER
(Theoretical Circuit)

both control and gate circuits. In case that the absolute values of the nonlinear terms $\rho_1 f_1(\phi_x, \phi_y)$ and $\rho_2 f_2(\phi_x, \phi_y)$ are less than that of the linear terms $(-\frac{1}{T_1}\phi_x + V_{1m}\sin\omega t + V_0)$ and $(-\frac{1}{T_2}\phi_y + V_{2m}\sin\omega t)$ respectively, equations (17) and (18) can be assumed to be quasi-linear. Since the nonlinear terms appear with small coefficients ρ_1 and ρ_2, the solutions of equations (17) and (18) can be expressed in the form of Poisson's series:

$$\phi_x = \phi_{x0} + \rho_1\phi_{x1} + \rho_1^2\phi_{x2} + \rho_1^3\phi_{x3} + \cdots \tag{32}$$

$$\phi_y = \phi_{y0} + \rho_2\phi_{y1} + \rho_2^2\phi_{y2} + \rho_2^3\phi_{y3} + \cdots \tag{33}$$

where ρ_1 and ρ_2 are given by equations (24) and (25) respectively.

Rearranging equations (32) and (33),

$$\phi_x = \phi_{x0} + \rho_1 [\text{illegible}] \cdots \tag{34}$$

$$\phi_y = \phi_{y0} + \rho_2 [\text{illegible}] \cdots \tag{35}$$

Substituting equations (32) and (35) into equations (17), (33) and (34) into equation (18) then equating terms containing the same powers of ρ_1 and ρ_2 respectively, the following series of linear differential equations are obtained:

$$\frac{d}{dt}\phi_{x0} + \frac{1}{T_1}\phi_{x0} = V_{1m}\sin\omega t + V_0 \tag{36}$$

$$\frac{d}{dt}\phi_{y0} + \frac{1}{T_2}\phi_{y0} = V_{2m}\sin\omega t \tag{37}$$

$$\frac{d}{dt}\phi_{x1} + \frac{1}{T_1}\phi_{x1} = f_1(\phi_{x0}, \phi_{y0}) \tag{38}$$

$$\frac{d}{dt}\phi_{y1} + \frac{1}{T_2}\phi_{y1} = f_2(\phi_{x0}, \phi_{y0}) \tag{39}$$

$$\frac{d}{dt}\phi_{x2} + \frac{1}{T_1}\phi_{x2} = [\text{illegible}] \tag{40}$$

$$\frac{d}{dt}\phi_{y2} + \frac{1}{T_2}\phi_{y2} = [\text{illegible}] \tag{41}$$

......

......

In the above equations, f_{ϕ_x} and f_{ϕ_y} are the partial derivatives of f with respect to ϕ_x and ϕ_y.

Equations (36) and (41) are linear. The first set of equations (36) and (37) can be easily solved for ϕ_{xo} and ϕ_{yo}. This solution is substituted into equations (38) and (39) which can then be solved for ϕ_{x1} and ϕ_{y1}. This solution is substituted into equations (40) and (41) to solve for ϕ_{x2} and ϕ_{y2}, and so on....In general the solution of kth set leads to the solution of the (k+1)th set.

In all cases in which convergence of Poisson's series given by equations (32) and (33) exists, the exact solution can be approached by reiteration of successive substitutions. The convergence of Poisson's series is proved in Appendix B. The additional term obtained by a further substitution is smaller than the previous one and ultimately further substitution leads only to a negligible correction. In many practical cases the respective first term ϕ_{xo} and ϕ_{yo} of equations (32) and (33) alone are sufficiently close to the exact answer. Such a solution is the first approximation solution. In the first approximation,

$$\phi_x = \phi_{xo} \tag{42}$$

$$\phi_y = \phi_{yo} \tag{43}$$

A closer solution can be obtained by taking the first two terms of the series (32) and (33), and the solution is called the second approximation. In the second approximation,

$$\phi_x = \phi_{xo} + \phi_{x1} \tag{44}$$

$$\phi_y = \phi_{yo} + \phi_{y1} \tag{45}$$

If a more exact solution is wanted, more terms in the series (32) and (33) should be taken, and the solution is denoted as kth approximation, in which,

$$\phi_x = \phi_{x0} + \rho_1 \phi_{x1} + \rho_1^2 \phi_{x2} + \cdots\cdots + \rho_1^{k-1} \phi_{x(k-1)} \qquad (46)$$

$$\phi_y = \phi_{y0} + \rho_2 \phi_{y1} + \rho_2^2 \phi_{y2} + \cdots\cdots + \rho_2^{k-1} \phi_{y(k-1)} \qquad (47)$$

3. <u>First approximation theory</u>.

For a practical application of the theory derived in the previous sections, and to simplify the equations without affecting seriously the exactness of the polynomial to the F, ϕ curve, it can be assumed that the magnetization characteristics of the core material can be approximated by a three term polynomial within its operating range,

$$F = k\,\phi + k_3\,\phi^3 + k_5\,\phi^5 \qquad \text{ampere-turn} \quad (48)$$

and that ρ_1 and ρ_2 are so small such that equations (32) and (33) can be approximated by

$$\phi_x = \phi_{xo} \qquad \text{weber} \quad (49)$$

$$\phi_y = \phi_{yo} \qquad \text{weber} \quad (50)$$

Evaluating ϕ_{xo} and ϕ_{yo} from equations (36) and (37), and substituting them into equations (49) and (50), the solution of fluxes of first approximation is obtained,

$$\phi_x = \phi_{ob} + \phi_{1m} \sin\,(\omega t - \theta_1) \qquad \text{weber} \quad (51)$$

$$\phi_y = \phi_{2m} \sin(\omega t - \theta_2) \qquad \text{weber} \quad (52)$$

where

$$\phi_{ob} = \frac{N_1 E_b}{k_1\ 2R_1} \qquad \text{weber} \quad (53)$$

$$\phi_{1m} = \frac{N_1}{k_1 \; 2R_1} \frac{E_{1m}}{\sqrt{(1 + (\frac{\Omega}{\Omega_0})^2}} \qquad \text{weber} \qquad (54)$$

$$\phi_{2m} = \frac{N_2}{k \; 2R_2} \frac{E_{2m}}{\sqrt{(1 + \frac{R_L}{2R_2})^2 + (\frac{\omega}{\omega_0})^2}} \qquad \text{weber} \qquad (55)$$

$$\theta_1 = \tan^{-1} \Omega/\Omega_0 \qquad \text{degree} \qquad (56)$$

$$\theta_2 = \tan^{-1} \omega/\omega_0 \qquad \text{degree} \qquad (57)$$

$$\Omega_0 = \frac{k_1 \; R_1}{N_1^2} \qquad \text{radian/sec} \qquad (58)$$

$$\omega_0 = \frac{k_1 \; R_2}{N_2^2} \qquad \text{radian/sec} \qquad (59)$$

Substituting equations (51) and (52) into equations (30) and (31)and letting n's be the odd numbers up to 5, the current responses of the first approximation attain the following terms:

$$\begin{aligned} i_1 = & \Big[I_{10} + I_{11} \sin(\Omega t - \theta_1) + I_{12} \cos 2(\Omega t - \theta_1) \\ & + I_{13} \sin 3(\Omega t - \theta_1) + I_{14} \cos 4(\Omega t - \theta_1) \\ & + I_{15} \sin 5(\Omega t - \theta_1) \Big] + \Big[I_{21} \sin(\Omega t - \theta_1) + I_{20} \\ & + I_{22} \cos 2(\Omega t - \theta_1) + I_{23} \sin 3(\Omega t - \theta_1) \Big] \cos 2(\omega t - \theta_2) \\ & + \Big[I_{40} + I_{41} \sin(\Omega t - \theta_1) \Big] \cos 4(\omega t - \theta_2) \quad \text{ampere} \end{aligned} \qquad (60)$$

$$\begin{aligned} i_2 = & \Big[I_{10} + I_{11} \sin(\Omega t - \theta_1) + I_{12} \cos 2(\Omega t - \theta_1) + I_{13} \sin 3(\Omega t - \theta_1) \\ & + I_{14} \cos 4(\Omega t - \theta_1) \Big] \sin(\omega t - \theta_2) + \Big[I_{30} + I_{31} \sin(\Omega t - \theta_1) \\ & + I_{32} \cos 2(\Omega t - \theta_1) \Big] \sin 3(\omega t - \theta_2) + I_{50} \sin 5(\omega t - \theta_2) \quad \text{ampere} \end{aligned} \qquad (61)$$

where the I's are given in Appendix C. If we consider the envelope of the modulated signal of only the fundamental carrier frequency across the load resistance, the output voltage will be:

$$e_o = R_L \Big[I_{11} \sin(\Omega t - \theta_1) + I_{12} \cos 2(\Omega t - \theta_1)$$
$$+ I_{13} \sin 3(\Omega t - \theta_1) + I_{14} \cos 4(\Omega t - \theta_1) \qquad (62)$$

The fundamental voltage gain is then:

$$K_v = \frac{R_L \, I_{11}}{E_{1m}} \qquad \text{dimensionless} \quad (63)$$

and the percentage harmonic distortion:

$$\%\ \text{2nd Harmonic distortion} = \frac{I_{12}}{I_{11}} \times 100 \qquad (64)$$

$$\%\ \text{3rd Harmonic distortion} = \frac{I_{13}}{I_{11}} \times 100\ \text{, etc.....} \qquad (65)$$

The phase difference between input voltage and the fundamental component of the output voltage is evidently θ_1.

4. <u>Fundamental voltage gain.</u>

From the value of I_{11} defined in equation (155) if:

$$E_{bo} = \frac{2R_1 k_1}{N_1} \sqrt{\frac{3}{10} \left| \frac{k_3}{k_5} \right|} \qquad \text{volts} \quad (66)$$

$$E_{1o} = \frac{2R_1 k_1}{N_1} \sqrt{\frac{1}{5} \left| \frac{k_3}{k_5} \right|} \qquad \text{volts} \quad (67)$$

$$E_{20} = \frac{2R_2 k_1}{N_2} \sqrt{\frac{1}{5} \left| \frac{k_1}{k_5} \right|} \qquad \text{volts} \quad (68)$$

$$A = 2.08 \frac{k_3^2}{k_1 k_5} \frac{N_1}{N_2} \frac{R_2}{R_1} \qquad \text{dimensionless} \quad (69)$$

the fundamental voltage gain derived in equation (63) can be expressed as:

$$K = \frac{A\left(\frac{E_2}{E_{20}}\right)\left(\frac{E_b}{E_{bo}}\right)\left(\frac{R_L}{2R_2}\right)}{\left[1+\left(\frac{\Omega}{\Omega_o}\right)^2\right]^{1/2}\left[\left(1+\frac{R_L}{2R_2}\right)^2+\left(\frac{\omega}{\omega_o}\right)^2\right]^{1/2}} \left[1-\left(\frac{E_b}{E_{bo}}\right)^2 - \frac{\left(\frac{E_1}{E_{10}}\right)^2}{1+\left(\frac{\Omega}{\Omega_o}\right)^2} - \frac{\left(\frac{E_2}{E_{20}}\right)^2}{\left(1+\frac{R_L}{2R_2}\right)^2+\left(\frac{\omega}{\omega_o}\right)^2}\right] \qquad (70)$$

where Ω_c and ω_c were defined in equations (58) and (59).

The equation (70) shows that this gain is a function of six dimensionless parameters:

$$\frac{E_b}{E_{bo}},\ \frac{E_1}{E_{10}},\ \frac{E_2}{E_{20}},\ \frac{R_L}{2R_2},\ \frac{\omega}{\omega_c} \text{ and } \frac{\Omega}{\Omega_c}$$

5. <u>Amplitude of voltage gain as a function of the dimensionless parameters:</u>

(a) <u>Gain as a function of bias</u> -

If everything is considered constant except E_b/E_{bo}, the gain may be expressed as:

$$K = \alpha_b \frac{E_b}{E_{bo}} \left[1 - \beta_b \left(\frac{E_b}{E_{bo}} \right)^2 \right] \tag{71}$$

where

$$\alpha_b = \frac{A\left(\frac{E_2}{E_{20}}\right)\left(\frac{R_L}{2R_2}\right)\left\{1-\left(\frac{E_1}{E_{10}}\right)^2\left[1+\left(\frac{\Omega}{\Omega_c}\right)^2\right]^{-1} - \left(\frac{E_2}{E_{20}}\right)^2\left[\left(1+\frac{R_L}{2R_2}\right)^2+\left(\frac{\omega}{\omega_c}\right)^2\right]^{-1}\right\}}{\left[1+\left(\frac{\Omega}{\Omega_c}\right)^2\right]^{1/2}\left[\left(1+\frac{R_L}{2R_2}\right)^2+\left(\frac{\omega}{\omega_c}\right)^2\right]^{1/2}} \tag{72}$$

and

$$\beta_b = \frac{1}{1-\left(\frac{E_1}{E_{10}}\right)^2\left[1+\left(\frac{\Omega}{\Omega_c}\right)^2\right]^{-1} - \left(\frac{E_2}{E_{20}}\right)^2\left[\left(1+\frac{R_L}{2R_2}\right)^2+\left(\frac{\omega}{\omega_c}\right)^2\right]^{-1}} \tag{73}$$

The theoretical characteristics gain curve as a function of bias is plotted in Fig. 3.

When the bias is zero, the signal voltage generates a corresponding flux in one direction in one half cycle, then in the other direction the following half cycle. The envelope of the modulated output is dominated by even harmonics. The fundamental gain is zero. Increasing the bias, which prevents the flux generated by the signal voltage from being of the reverse direction, results in an increase of fundamental gain and decrease of even harmonic distortion. If the bias is further increased, the second order term in the bracket of equation (71) becomes significant and K will

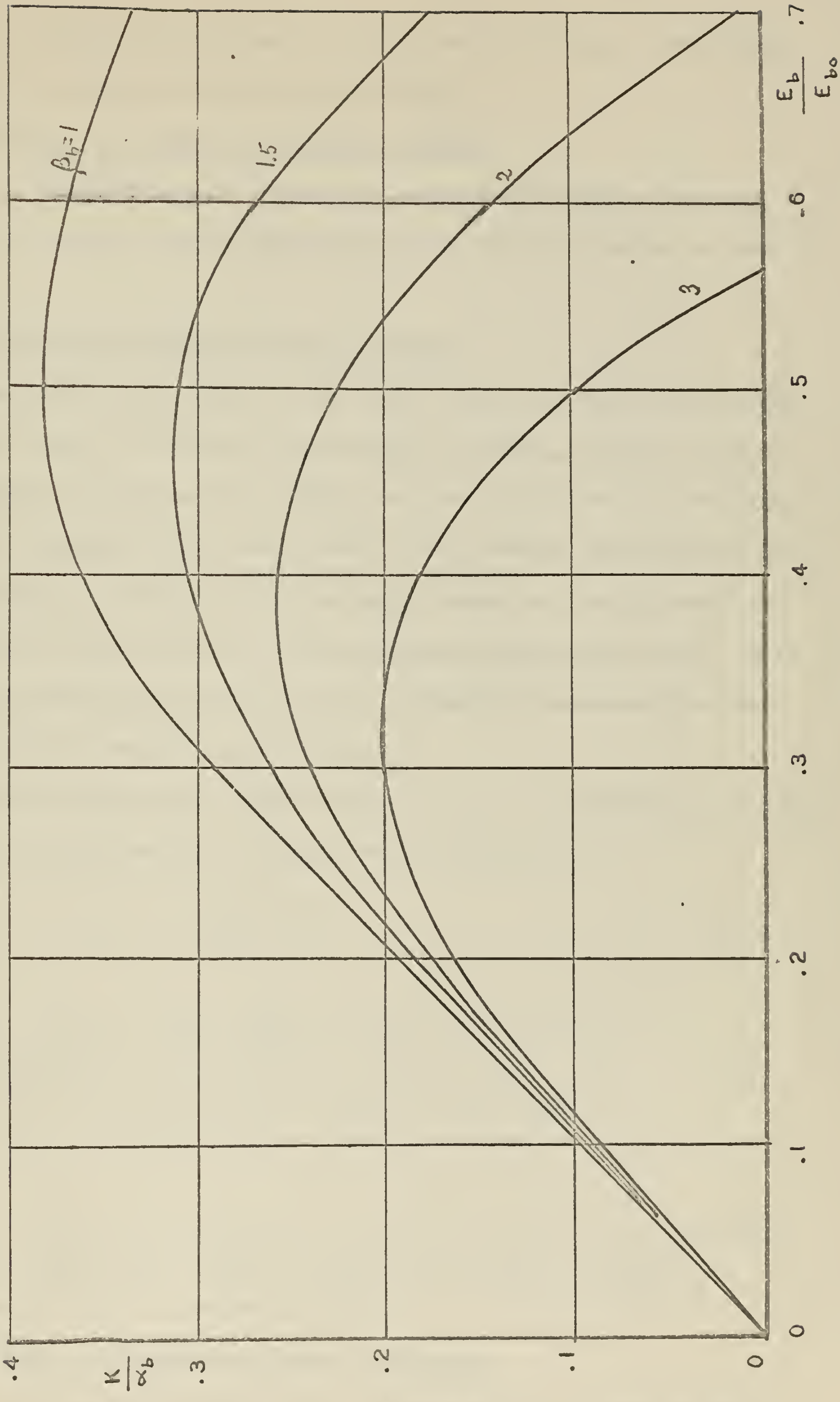

FIG. 3 - GAIN V/S BIAS

(Theoretical)

decrease. Therefore the curve of the gain will bend down. Physically, it means that the bias has caused saturation.

(b) Gain as a function of carrier voltage-

The amplitude of the carrier voltage will produce the same effect as the bias. The characteristic gain curve is similar to that of Fig. 3.

(c) Gain as a function of input voltage -

The gain is independent of the input voltage as long as this input voltage is small. When the input voltage increases, the third term in the bracket of equation (70) E_1^2/E_{10}^2 becomes significant in comparison with the summation of the other terms in the bracket, therefore the gain will decrease. Physically the flux swing caused by a large signal voltage covers a large portion on the nonlinear magnetization curve. More harmonics are thus generated while the fundamental component does not increase proportionally with the input.

If the dimensionless input voltage E_1/E_{10} is considered as the only variable in equation (70), the gain may be expressed as:

$$K = \alpha_1 \left[1 - \beta_1 \left(\frac{E_1}{E_{10}} \right)^2 \right] \tag{74}$$

where

$$\alpha_1 = \frac{A \left(\frac{E_2}{E_{20}} \right) \left(\frac{R_L}{2R_2} \right)^2 \left\{ 1 - \left(\frac{E_b}{E_{b0}} \right)^2 - \left(\frac{E_2}{E_{20}} \right)^2 \left[\left(1 + \frac{R_L}{2R_2} \right)^2 + \left(\frac{\omega}{\omega_0} \right)^2 \right]^{-1} \right\}}{\left[1 + \left(\frac{\Omega}{\Omega_0} \right)^2 \right]^{1/2} \left[\left(1 + \frac{R_L}{2R_2} \right)^2 + \left(\frac{\omega}{\omega_0} \right)^2 \right]^{1/2}} \tag{75}$$

and

$$\beta_1 = \frac{1}{\left[1 + \left(\frac{\Omega}{\Omega_0} \right)^2 \right] \left\{ 1 - \left(\frac{E_b}{E_{b0}} \right)^2 - \left(\frac{E_2}{E_{20}} \right)^2 \left[\left(1 + \frac{R_L}{2R_2} \right)^2 + \left(\frac{\omega}{\omega_0} \right)^2 \right]^{-1} \right\}} \tag{76}$$

Equation (74) is plotted in Fig. 4.

(d) Gain as a function of signal frequency -

If the dimensionless signal frequency Ω/Ω_0 is considered as the only variable in equation (70), the gain will be expressed as:

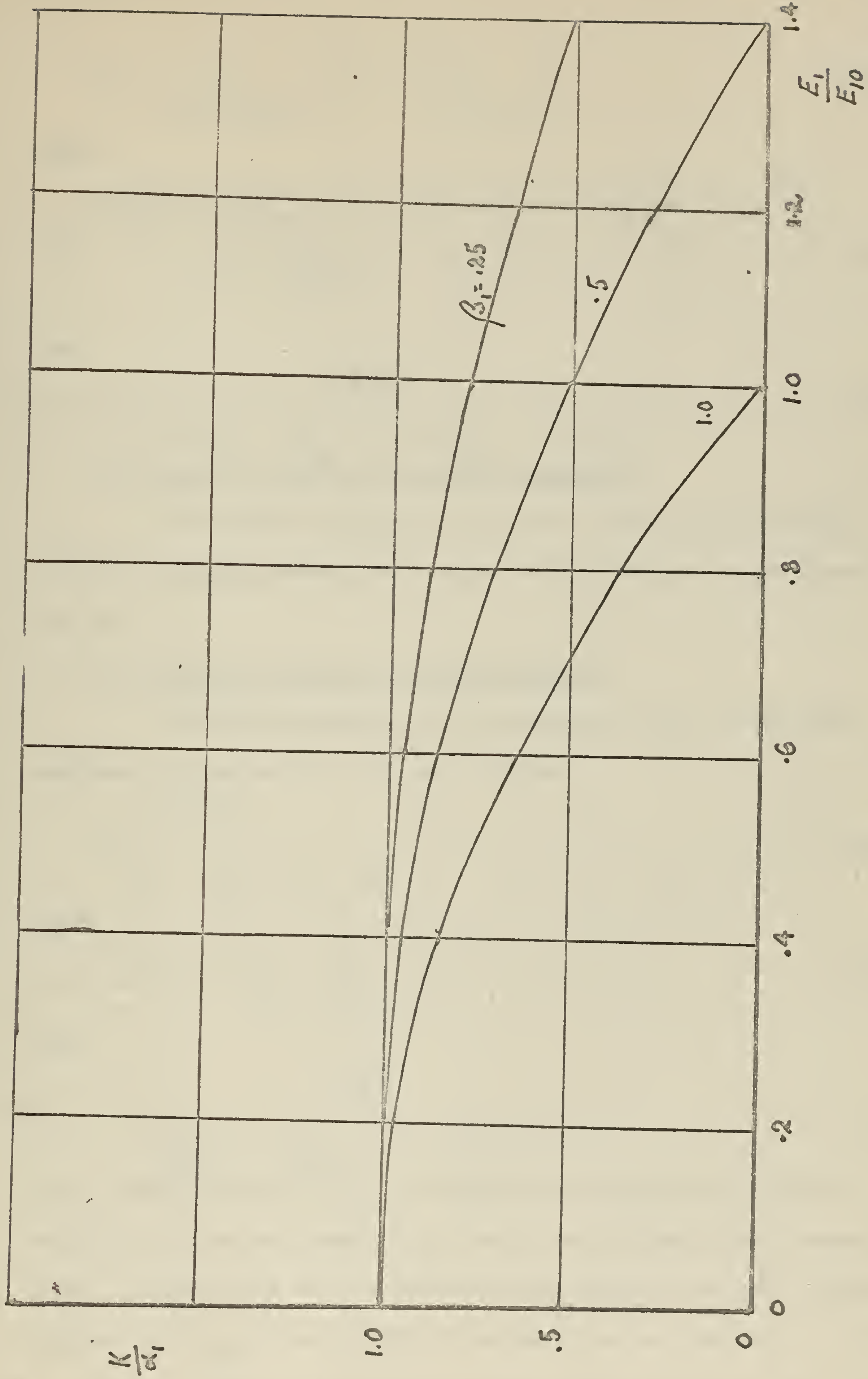

FIG. 4 - GAIN V/S INPUT

(Theoretical)

$$K = \frac{\alpha_{\Omega}}{\left[1+\left(\frac{\Omega}{\Omega_c}\right)^2\right]^{1/2}}\left[1-\frac{\beta_{\Omega}}{1+\left(\frac{\Omega}{\Omega_c}\right)^2}\right] \tag{77}$$

where

$$\alpha_{\Omega} = \frac{A\left(\frac{E_2}{E_{2c}}\right)\left(\frac{E_b}{E_{bc}}\right)\left(\frac{R_L}{2R_2}\right)\left\{1-\left(\frac{E_b}{E_{bc}}\right)^2-\left(\frac{E_2}{E_{2c}}\right)^2\left[\left(1+\frac{R_L}{2R_2}\right)^2+\left(\frac{\omega}{\omega_0}\right)^2\right]^{-1}\right\}}{\left[\left(1+\frac{R_L}{2R_2}\right)^2+\left(\frac{\omega}{\omega_0}\right)^2\right]^{1/2}} \tag{78}$$

and

$$\beta_{\Omega} = \frac{\left(\frac{E_1}{E_{1c}}\right)^2}{1-\left(\frac{E_b}{E_{bc}}\right)^2-\left(\frac{E_2}{E_{2c}}\right)^2\left[\left(1+\frac{R_L}{2R_2}\right)^2+\left(\frac{\omega}{\omega_0}\right)^2\right]^{-1}} \tag{79}$$

(e) Gain as a function of carrier frequency -

The carrier frequency has a similar effect upon the gain. Plotted, the gain characteristic curve will be similar to the curve in Fig. 5.

(f) Gain as a function of load resistance -

If the dimensionless load resistance $R_{L/2R_2}$ is the only variable in equation (70), the gain will be:

$$K = \frac{\alpha_L\left(\frac{R_L}{2R_2}\right)}{\left[\left(1+\frac{R_L}{2R_2}\right)^2+\left(\frac{\omega}{\omega_0}\right)^2\right]^{1/2}}\left[1-\frac{\beta_L}{\left(1+\frac{R_L}{2R_2}\right)^2+\left(\frac{\omega}{\omega_0}\right)^2}\right] \tag{80}$$

where

$$\alpha_L = \frac{A\left(\frac{E_2}{E_{2c}}\right)\left(\frac{E_b}{E_{bc}}\right)\left\{1-\left(\frac{E_b}{E_{bc}}\right)^2-\left(\frac{E_1}{E_{1c}}\right)^2\left[1+\left(\frac{\Omega}{\Omega_c}\right)^2\right]^{-1}\right\}}{\left[1+\left(\frac{\Omega}{\Omega_c}\right)^2\right]^{1/2}} \tag{81}$$

and

$$\beta_L = \frac{\left(\frac{E_2}{E_{2c}}\right)^2}{1-\left(\frac{E_b}{E_{bc}}\right)^2-\left(\frac{E_1}{E_{1c}}\right)^2\left[1+\left(\frac{\Omega}{\Omega_c}\right)^2\right]^{-1}} \tag{82}$$

For a definite value of ω/ω_0, the gain curve is plotted in Fig. 6. According to the gain equation (Eq. 80), the gain would reach asymptotically a finite value as load resistance increases to infinity. However physically the gain is expected to approach zero as load goes to infinity.

When R_L goes to infinity, the gate circuit acts as an open circuit,

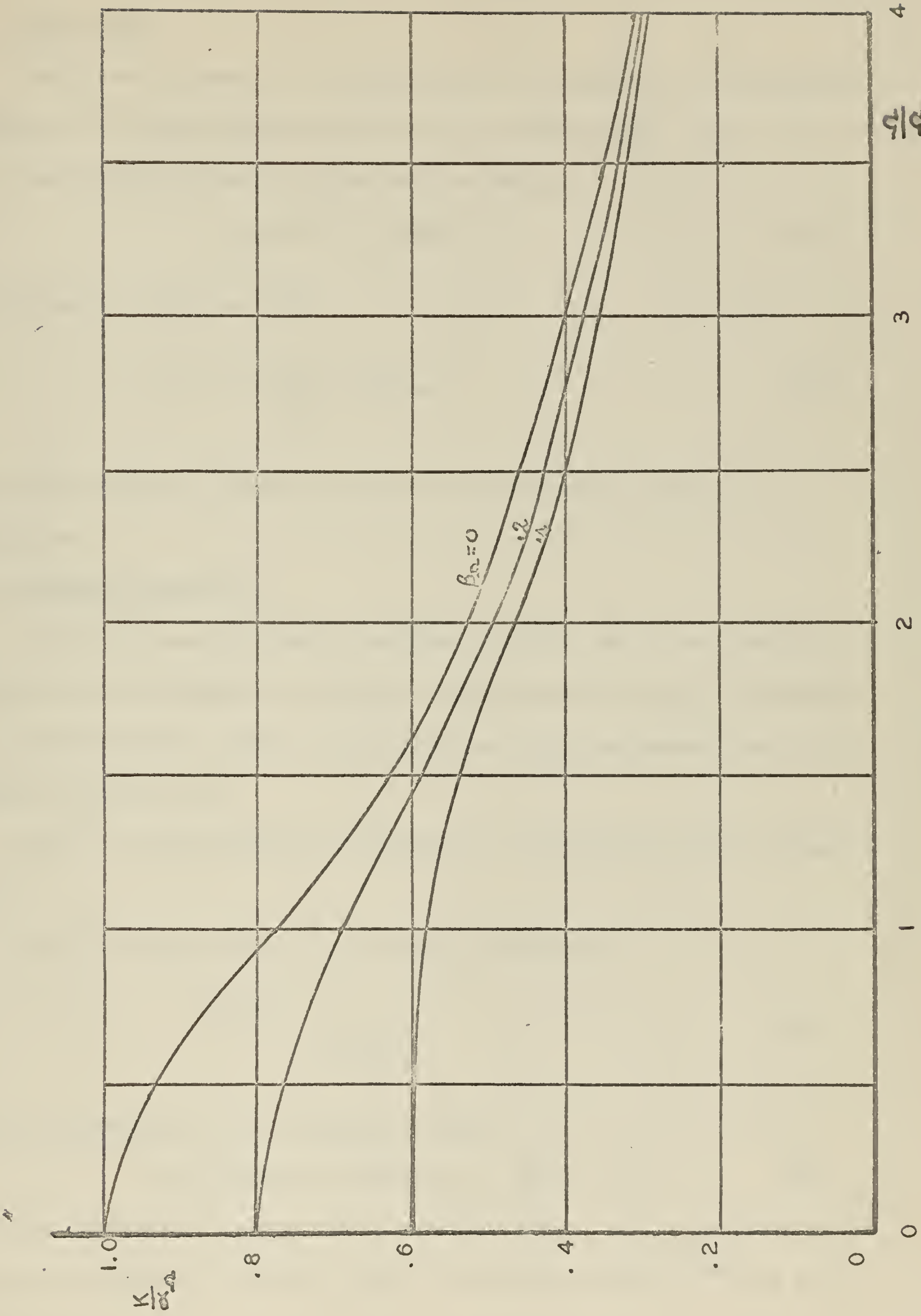

FIG. 5 - GAIN V/S SIGNAL FREQUENCY

(Theoretical)

and $E_o = E_m \sin \omega t$. $K_v = \frac{\partial E_o}{\partial E_{in}} = 0$

since E_o is independent of E_{in} which drives the core into saturation.

6. Phase angle -

The phase difference θ_1 between input voltage and the fundamental component of output appears implicitly in equation (62). Let L_{10} be the linearized inductance of the input winding,

$$L_{10} = N_1^2 / k_1 \text{ henry} \tag{83}$$

From equations (56) and (58)

$$\theta_1 = \tan^{-1} \frac{L_{10}}{R_1} \text{ degree} \tag{84}$$

The phase difference between input current and output current is negligible.

7. Harmonic distortion.

(a) In the output voltage equation (Eq. 62), the first term $R_L I_{11}$ represents the fundamental component, the second term $R_L I_{12}$ represents the second harmonic content, the third term $R_L I_{13}$ represents the third harmonic content etc.

Only the second harmonic distortion is considered in this presentation.

Let the second harmonic generation be defind as:

$$K^{2nd} = \frac{I_{12} R_L}{E_{1m}} \tag{85}$$

or as a percentage of the fundamental gain:

$$\% \text{ 2nd harmonic distortion} = \frac{K^{2nd}}{K} \times 100 \tag{86}$$

K is the fundamental gain given by equation (70). If I_{12} is substituted by its value given in equation (156) into equation (85), K^{2nd} may be expressed as:

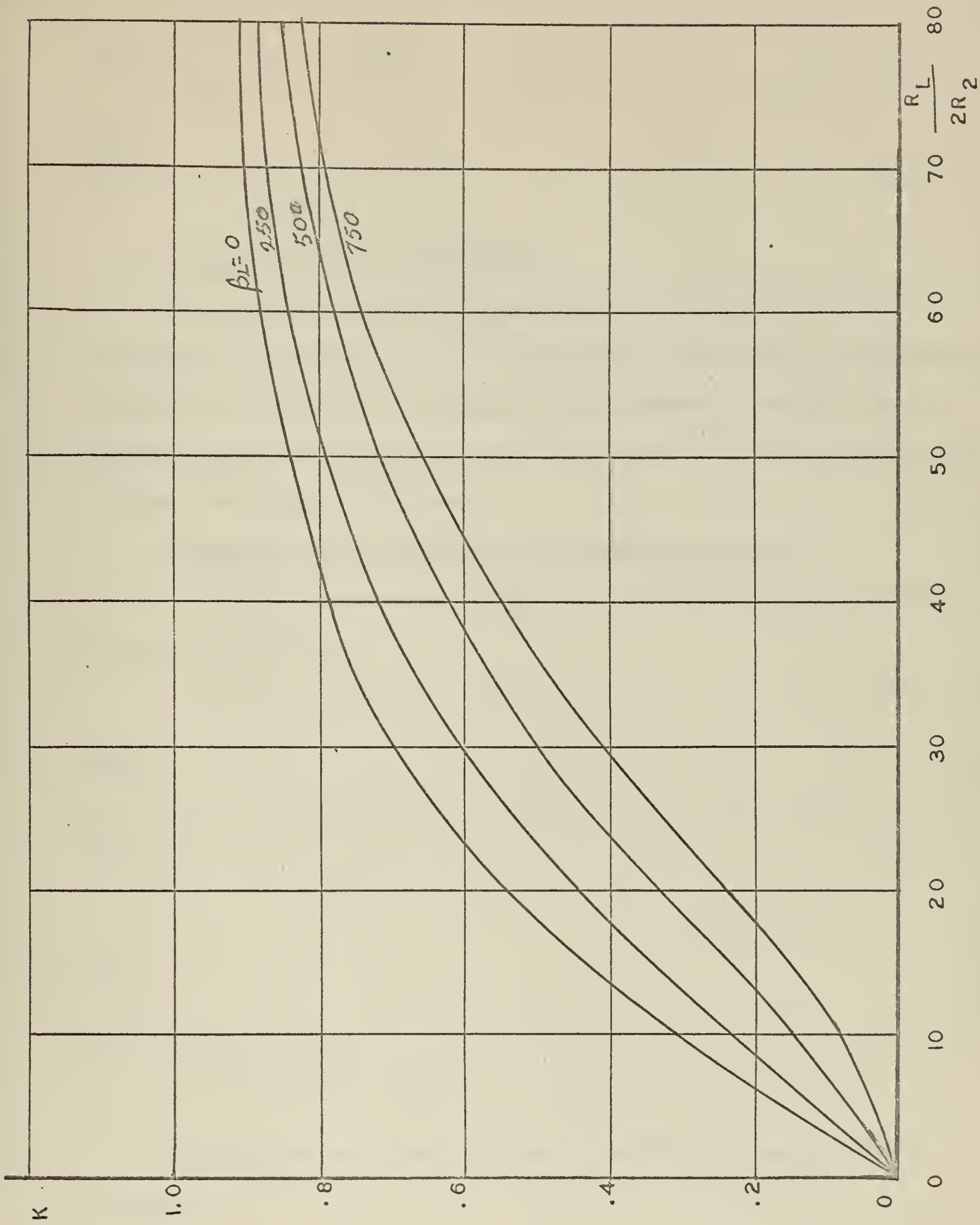

FIG. 6 – GAIN V/S LOAD RESISTANCE

(Theoretical)

$$K^{2nd} = \frac{A^{2nd}\left(\frac{E_2}{E_{ao}}\right)(\ldots)\left(\frac{R_L}{2R_2}\right)}{[\text{illegible}]}\left[\left(1-3\frac{E_b}{E_{bo}}\right) - \frac{2}{3}\,\frac{(\ldots)^2}{1+[\text{illegible}]} - \frac{[\text{illegible}]}{[\text{illegible}]}\right] \quad (87)$$

where

$$A^{2nd} = [\text{illegible}] \quad (88)$$

(b) <u>Effect of bias on K and K^{2nd}</u> -

From equations (70) and (87) and from Fig. 3 and 7, it is seen that as bias approaches zero, K^{2nd} approaches a finite value and K approaches zero. In the limit, the absence of the fundamental frequency and a maximum second harmonic in the output are expected. In fact, when the bias is zero, odd harmonics are absent.

(c) <u>Second harmonic generation as a function of bias</u> -

If the dimensionless E_b/E_{bo} is considered as the only variable equation (87) becomes:

$$K^{2nd} = \alpha_b^{2nd}\left[1 - \beta_b^{2nd}\left(\frac{E_b}{E_{bo}}\right)^2\right] \quad (89)$$

where

$$\alpha_b^{2nd} = [\text{illegible}] \quad (90)$$

and

$$\beta_b^{2nd} = [\text{illegible}] \quad (91)$$

The second harmonic generation as a function of bias is plotted in Fig. 7.

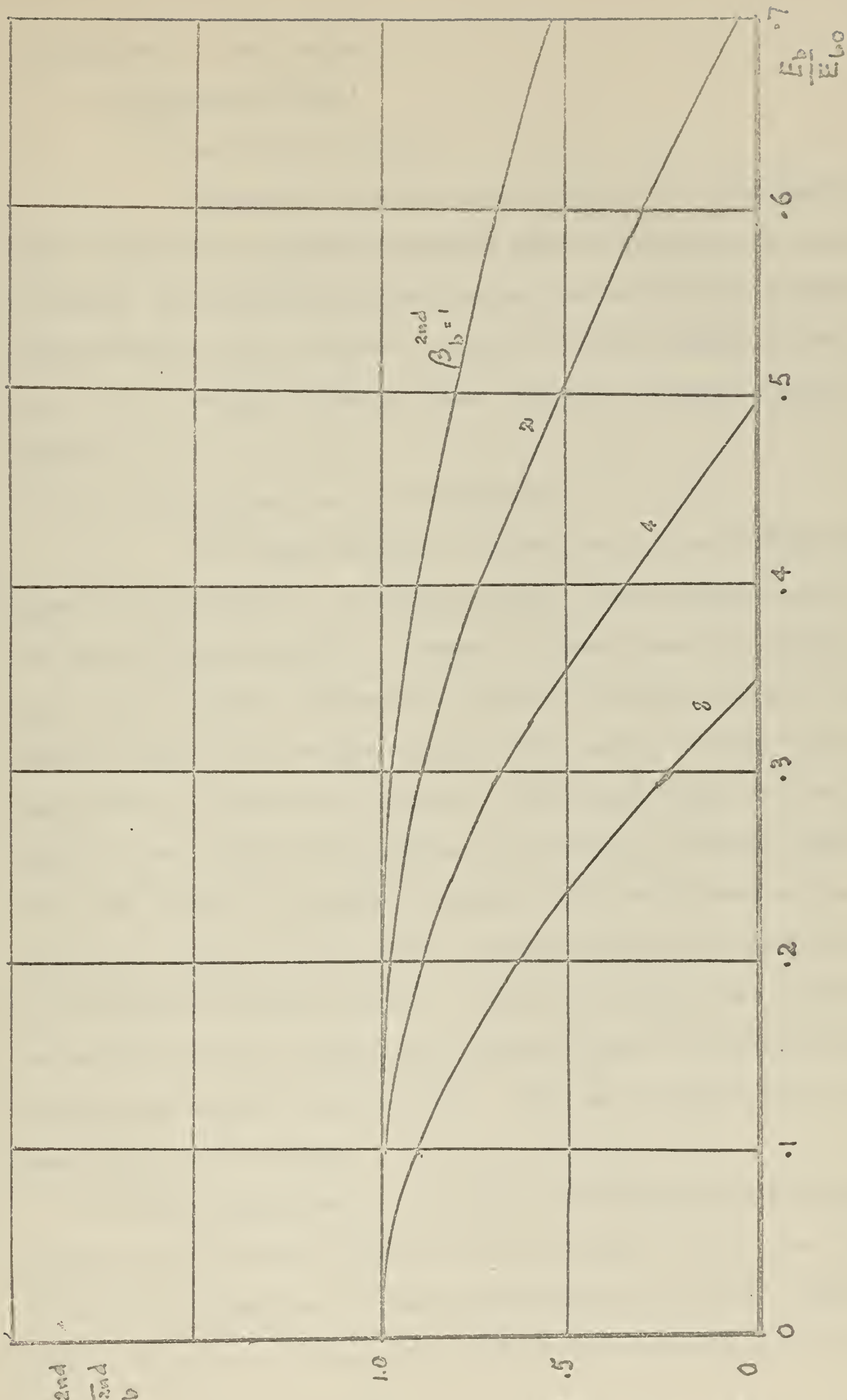

FIG. 7 - SECOND HARMONIC GENERATION

PLOTTED AGAINST BIAS (Theoretical)

III-Experimental Verification -

1. Experimental setup -

(a) Experimental circuit -

The circuit used for this experiment is illustrated in Figs. 1 and 2. Two identical saturable magnetic reactors are connected in series. An alternating current voltage source biased by a direct current voltage source was used to provide the input signal to the circuit. An a c voltage source of higher frequency was used as carrier supply.

(b) Equipment and instrumentation -

The cores used were a matched pair of core #50106 (HYMU80, Magnetic INC. Products). An Hewlett-Packard audio generator type HP 202A was used as signal generator. Between the signal generator and the input circuit a cathode follower was connected so that negligible impedance has been added to the control circuit. The cathode follower used in this experiment is illustrated in Fig. 18. The carrier supply for the magnetic amplifier was taken from the 400 cycle per second, 120 volt, 2-phase laboratory bus, through a powerstat to control the carrier voltage. The bias voltage was supplied by a 6 volt d c source through slide wire resistor to provide bias voltage desired. A slide wire resistor was connected in series with the bias source to keep the resistance of the control circuit constant for different bias voltages. The load resistance used was another slide wire resistor.

The cores were wound with 75 turns of AWG#38 wire for the control circuit and 500 turns of AWG#41 wire for the gate circuit. The load voltage was displayed on a Tektronix Oscilloscope Type 545, using type K plug-in amplifier for single trace and type CA plug-in unit for dual trace.

An General Radio Wave Analyzer type 736-A was used to measure the magnitude of the second harmonic in the output current.

(c) Magnetization curve of the magnetic reactor -

The magnetization characteristics of the saturable magnetic reactor were measured by using the circuit arranged as shown in Fig.8. The display of the X axis of the oscilloscope measures the magnetomotive force F and

$$F = \frac{V_x}{r_1} N_1 \qquad \text{ampere-turns} \qquad (92)$$

The Y axis measures the total flux when the values of r_2 and C_2 are so designed that

$$r_2 \gg \frac{1}{\omega C_2} \qquad \text{ohms} \qquad (93)$$

where ω is the frequency of the power supply.

Since the voltage equation of the secondary winding of the reactor (Fig. 8) is

$$N_2 \frac{d\phi}{dt} = i_2 r_2 + \frac{1}{C_2} \int i_2 dt. \qquad (94)$$

According to the relationship (93), the reactance drop in equation (94) can be neglected without introducing serious error, thus

$$i_2 = \frac{N_2}{r_2} \frac{d\emptyset}{dt} \qquad (95)$$

The voltage applied to the Y axis of the oscilloscope is

$$V_y = \frac{1}{C_2} \int i_2 \, dt \qquad (96)$$

Substituting the value of i_2 in equation (95) into equation (96),

$$\emptyset = \frac{r_2 C_2}{N_2} V_y \qquad \text{weber} \qquad (97)$$

Equation (97) shows that the total flux is proportional to the display of the Y axis of the oscilloscope. Thus the magnetization curve of the saturable reactor can be obtained simply by calibrating the oscilloscope. The magnetization characteristics of the reactors used in this experiment are shown in Fig. 9.

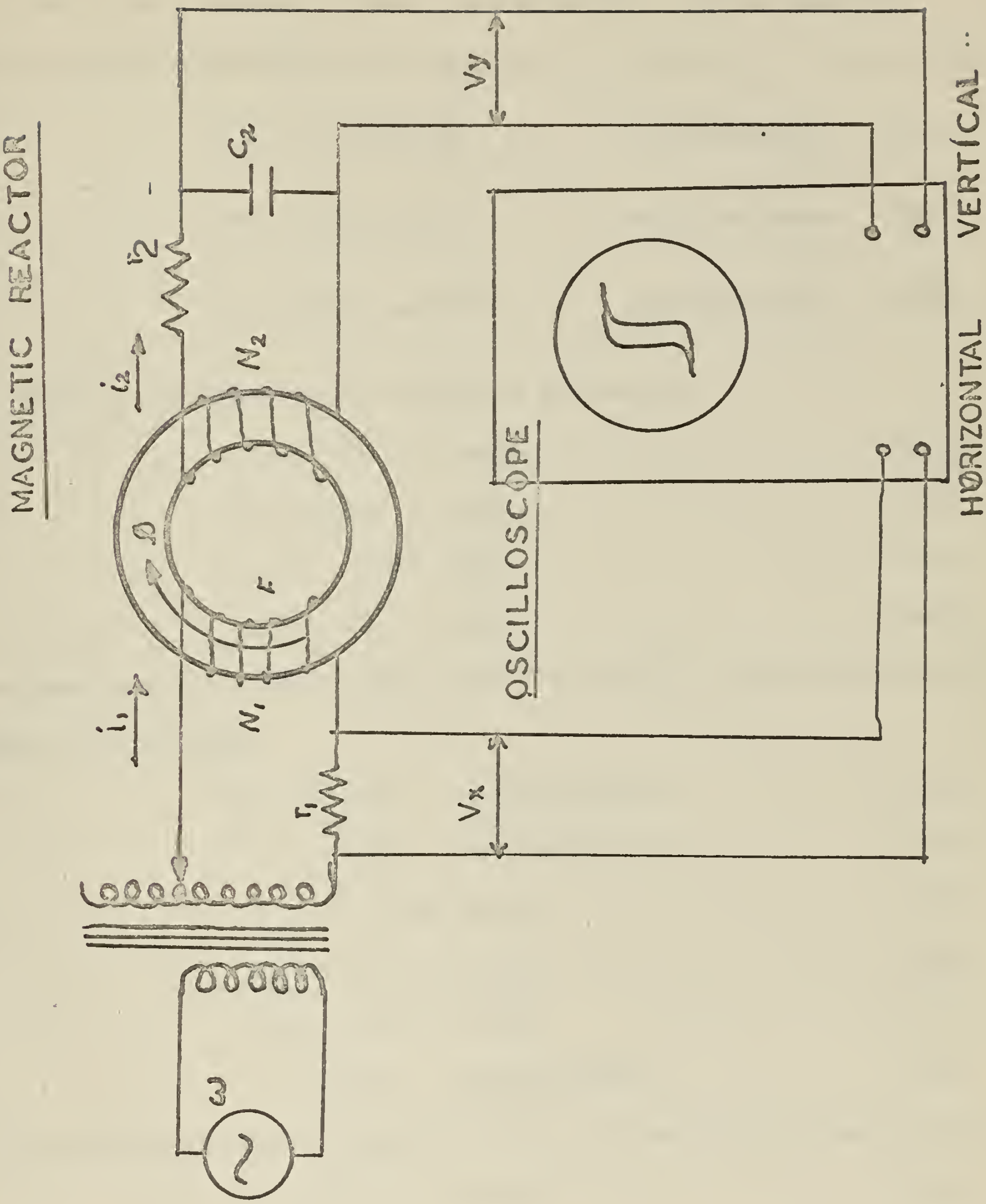

FIG. 8 - Circuit for measuring the magnetization characteristics of the Magnetic Reactors

(d) Computation

The magnetization curve shown in Fig. 9 may be represented by a three-term polynomial given in equation (48). Using numerical analysis method to determine the value of k_1, k_2, and k_3, there results

$$k_1 = .177 \times 10^6 \quad \text{amp-turns/weber} \qquad (98)$$

$$k_2 = -11.6 \times 10^{12} \quad \text{amp-turns/weber} \qquad (99)$$

$$k_3 = 348 \times 10^{18} \quad \text{amp-turns/weber} \qquad (100)$$

The magnetic amplifier has the following constants:

$$N_1 = 75 \quad \text{turns} \qquad (101)$$

$$N_2 = 500 \quad \text{turns} \qquad (102)$$

$$R_1 = 6.05 \quad \text{ohms} \qquad (103)$$

$$R_2 = 113 \quad \text{ohms} \qquad (104)$$

From equations (58), (59), (66), (67), (68) and (69), the following constants are evaluated:

$$\Omega_c = 196 \quad \text{radians/second} \qquad (105)$$

$$\omega_o = 80 \quad \text{radians/second} \qquad (106)$$

$$E_{bo} = 2.85 \quad \text{volts} \qquad (107)$$

$$E_{1o} = 2.32 \quad \text{volts} \qquad (108)$$

$$E_{20} = 6.5 \quad \text{volts} \qquad (109)$$

$$A = 12.8 \quad \text{dimensionless} \qquad (110)$$

If the following specific numerical values are used for the computations,

$$E_2 = 95 \quad \text{volts} \qquad (111)$$

$$\omega = 2\pi \times 400 \quad \text{radians/second} \qquad (112)$$

$$E_1 = 1.00 \quad \text{volt} \qquad (113)$$

$$\Omega = 2\pi \times 20 \quad \text{radians/second} \qquad (114)$$

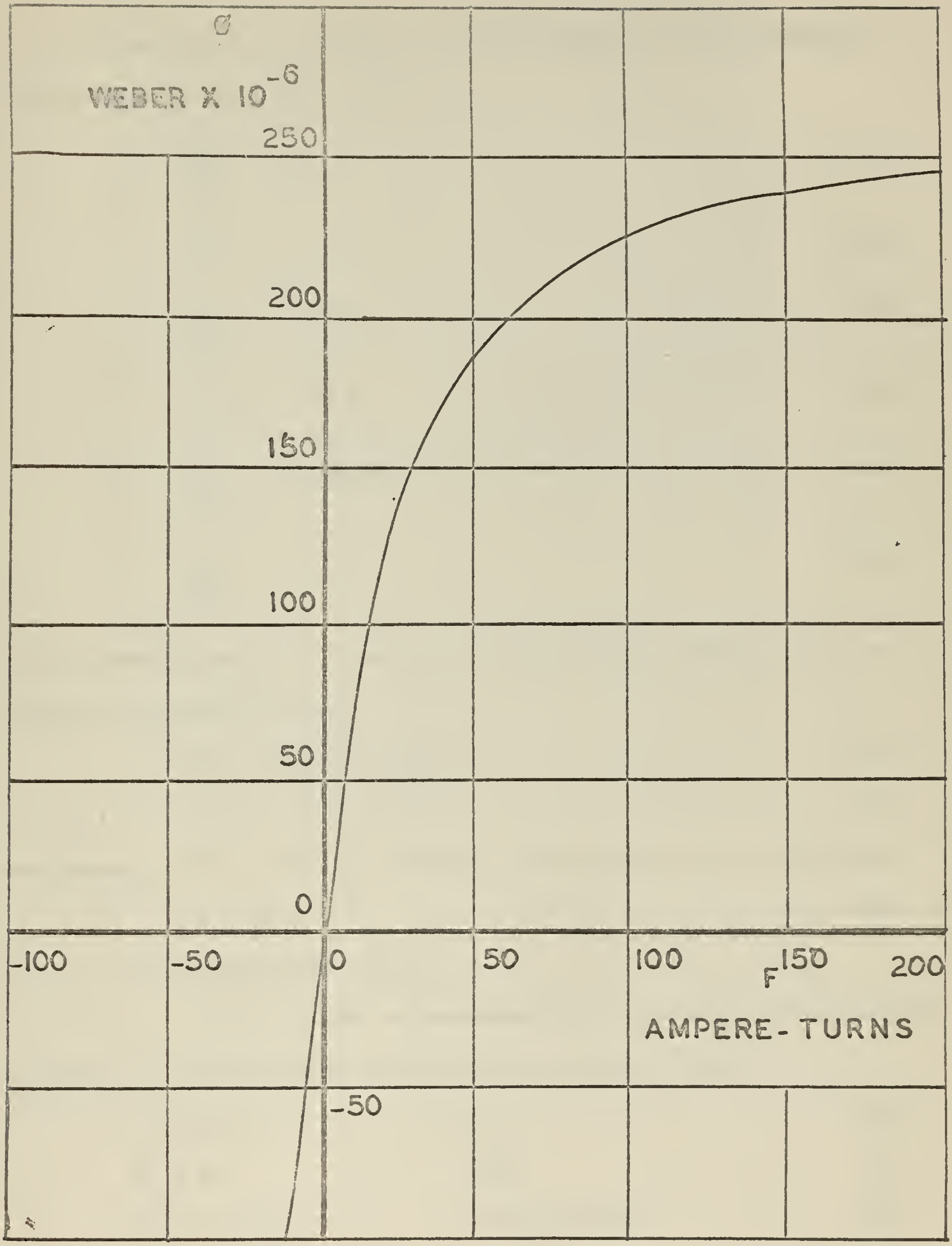

FIG. 9 - MAGNETIZATION CHARACTERISTICS of the reactors used in this experiment

$$E_b = 1.46 \quad \text{volts} \tag{115}$$

$$R_L = 5000 \quad \text{ohms} \tag{116}$$

the six dimensionless parameters which are present in the fundamental voltage gain equation (Eq. 70) will be:

$$\frac{E_2}{E_{20}} = 14.4 \tag{117}$$

$$\frac{\omega}{\omega_o} = 31.4 \tag{118}$$

$$\frac{E_1}{E_{10}} = 0.43 \tag{119}$$

$$\frac{\Omega}{\Omega_o} = 0.64 \tag{120}$$

$$\frac{E_b}{E_{bo}} = (0.512) \tag{121}$$

$$\frac{R_L}{2R_2} = 22 \tag{122}$$

and the coefficients ρ_1 and ρ_2 of the nonlinear factors given by equations (24) and (25) are:

$$\rho_1 = -0.54 \times 10^{-3} \tag{123}$$

$$\rho_2 = -5.20 \times 10^{-3} \tag{124}$$

From equation (70), the gain of first approximation can be calculated:

$$K = 24.14 \tag{125}$$

(e) Experimental results -

Fig. 11 shows the waveforms of the envelope of the output currents for different biases with other parameters being:

$$E_1 = 1.0 \quad \text{volt} \tag{126}$$

$$E_2 = 95 \quad \text{volts} \tag{127}$$

$$\Omega = 2 \times 20 \quad \text{radians/second} \tag{128}$$

$$\omega = 2 \times 400 \quad \text{radians/second} \tag{129}$$

$$R_L = 5000 \quad \text{ohms} \tag{130}$$

FIG. 10 - EXPERIMENTAL SET-UP

and the calibration of the oscilloscope being 8 volts per small division of the screen of the oscilloscope.

With E_b = 1.46 volt for example, the peak to peak of the modulating fundamental covers 8.1 small divisions. Thus the gain is

$$K = \frac{8.1 \times 8}{2 \times \sqrt{2} \times 1.0} = 23.0 \qquad (131)$$

From equations (72) and (73),

$$\alpha_b = 63 \qquad (132)$$

$$\beta_b = 1.48 \qquad (133)$$

From equations (131) and (132),

$$\frac{K}{\alpha_b} = 0.365 \qquad (134)$$

Since the constant E_{bo} = 2.85 volts (Eq. 107) and the bias voltage E_b = 1.46 volt,

$$\frac{E_b}{E_{bo}} = \frac{1.46}{2.85} = 0.512 \qquad (135)$$

By equations(134)and (135), this particular experimental result can be plotted with K/α_b as ordinate and E_b/E_{bo} as abcissa for the experimental curve of gain versus bias. (Fig. 12).

Fig. 11 (d) shows negligible second harmonic distortion, however, in the case of zero bias (Fig. 11 a), the modulating wave is dominated by second harmonic, which covers approximately 1.6 small division of the screen of the oscilloscope. Then

$$K^{2nd} = \frac{1.6 \times 8}{2 \times \sqrt{2} \times 1.0} = 4.57 \qquad (136)$$

From equations (90) and (91)

$$\alpha_b^{2nd} = 6.1 \qquad (137)$$

$$\beta_b^{2nd} = 3.9 \qquad (138)$$

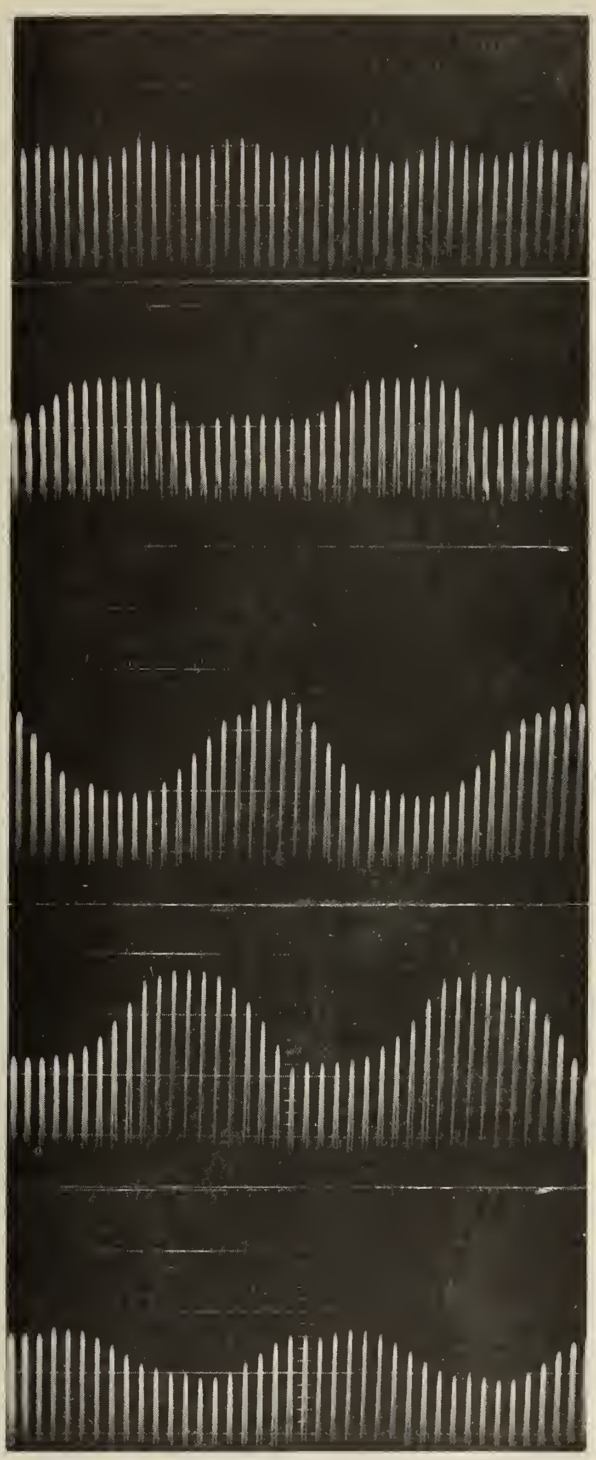

(a) E_b = 0 volt

(b) E_b = .485 volt

(c) E_b = .73 volt

(d) E_b = 1.46 volt

(e) E_b = 2.42 volts

FIG. 11 - ENVELOPES OF OUTPUT CURRENTS FOR DIFFERENT BIASES

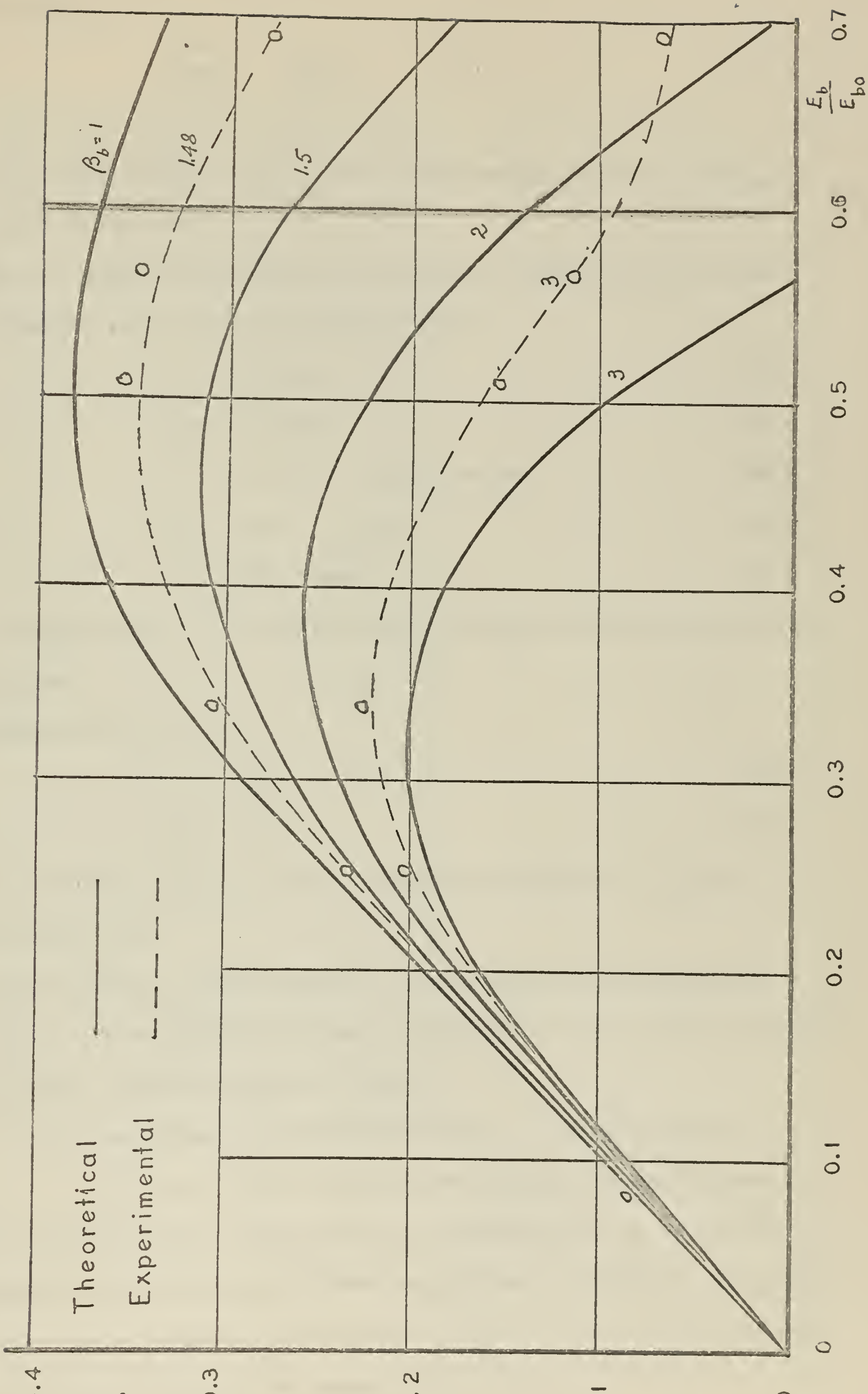

FIG. 12 - GAIN V/S BIAS

Thus for $E_b/E_{bo} \simeq 0$

$$\frac{K^{2nd}}{\alpha_b^{2nd}} = \frac{4.57}{6.1} = 0.75 \tag{139}$$

Different values of K^{2nd}/α_b^{2nd} with corresponding values of E_b/E_{bo} are plotted in Fig. 12.

Fig. 13 shows the envelopes of the output currents for different signal frequencies with other parameters being

$$E_1 = 1.0 \text{ volts} \tag{140}$$

$$E_2 = 95 \text{ volts} \tag{141}$$

$$\omega = 2\pi \times 400 \text{ radians/second} \tag{142}$$

$$E_b = 1.46 \text{ volt} \tag{143}$$

$$R_L = 5000 \text{ ohms} \tag{144}$$

and calibration being 6 volts per small division of the screen of the oscilloscope.

From equation (78) and (79)

$$\alpha_\Omega = 32 \tag{145}$$

$$\beta_\Omega = 0.3 \tag{146}$$

Different values of K/α_Ω with corresponding values of Ω/Ω_c are plotted in Fig. 14.

Fig. 15 shows the envelopes of output currents for different load resistances. An experimental curve is obtained in Fig. 16 with different values of K/α_L plotted against $R_L/2R_2$.

(f) Comparison of experimental results with computation

In Fig. 11 (Gain versus bias), the theoretical curves approach zero much more rapidly than the experimental ones if the bias is brought up into the region of over-saturation. A deviation is expected in this region where the three-term polynomial given in equation (48) does not closely represent the magnetization curve.

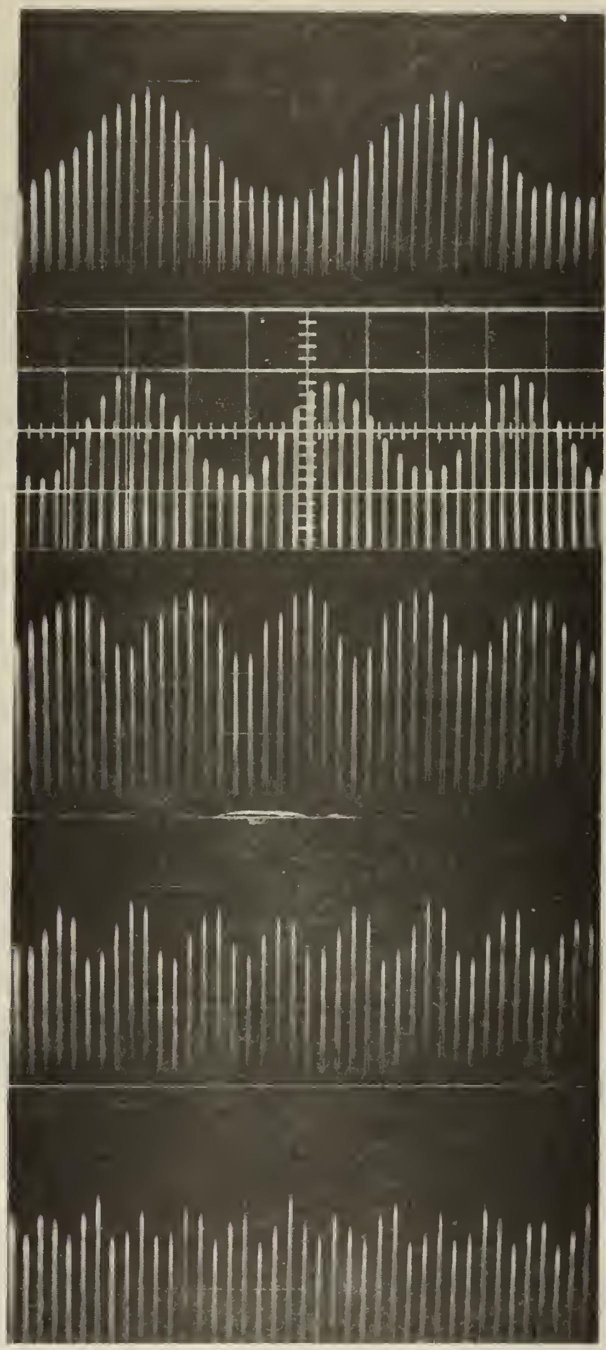

(a) $\Omega = 2\pi \times 20$

(b) $\Omega = 2\pi \times 30$

(c) $\Omega = 2\pi \times 50$

(d) $\Omega = 2\pi \times 80$

(e) $\Omega = 2\pi \times 120$

FIG. 13 - ENVELOPES OF OUTPUT CURRENTS FOR DIFFERENT SIGNAL FREQUENCIES

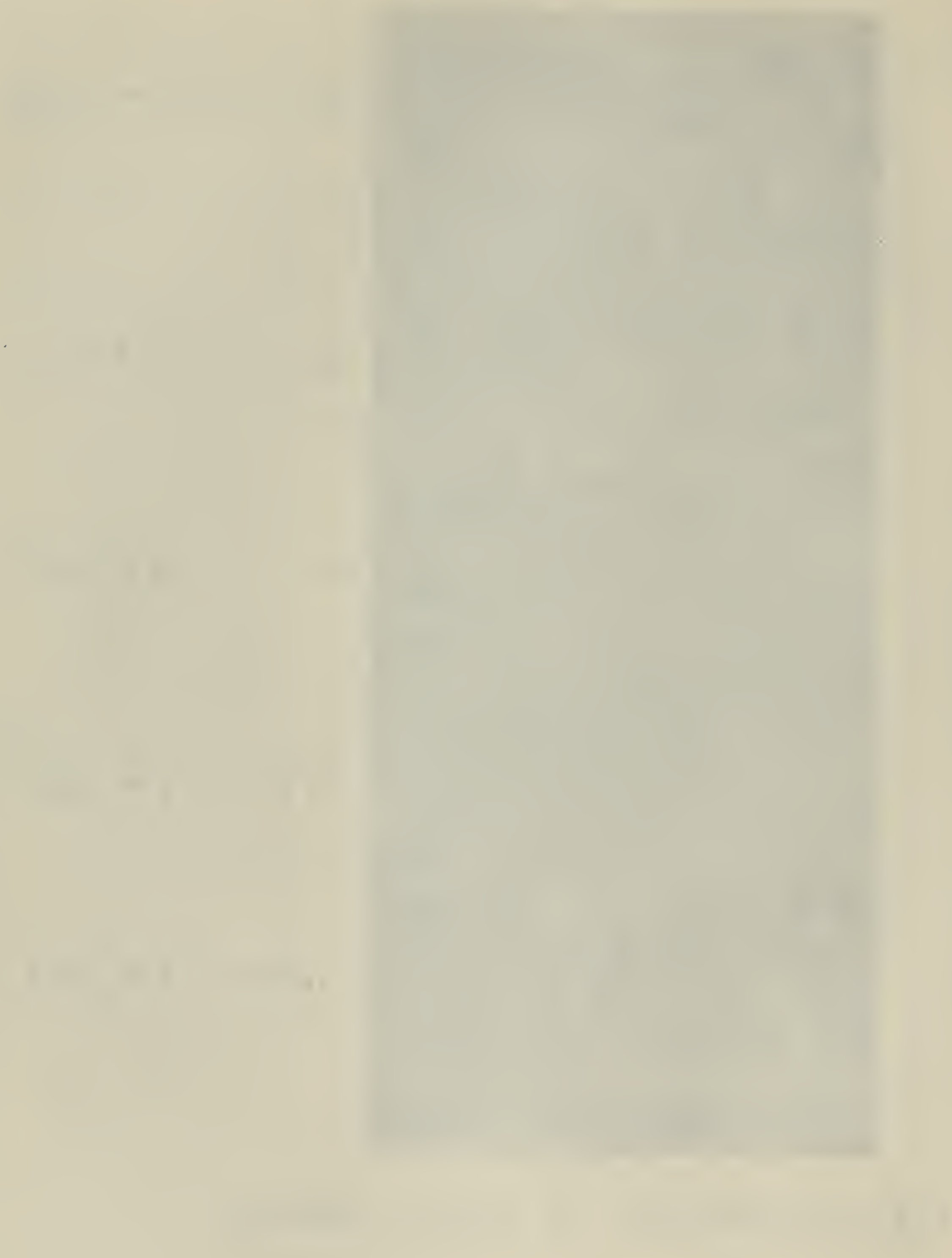

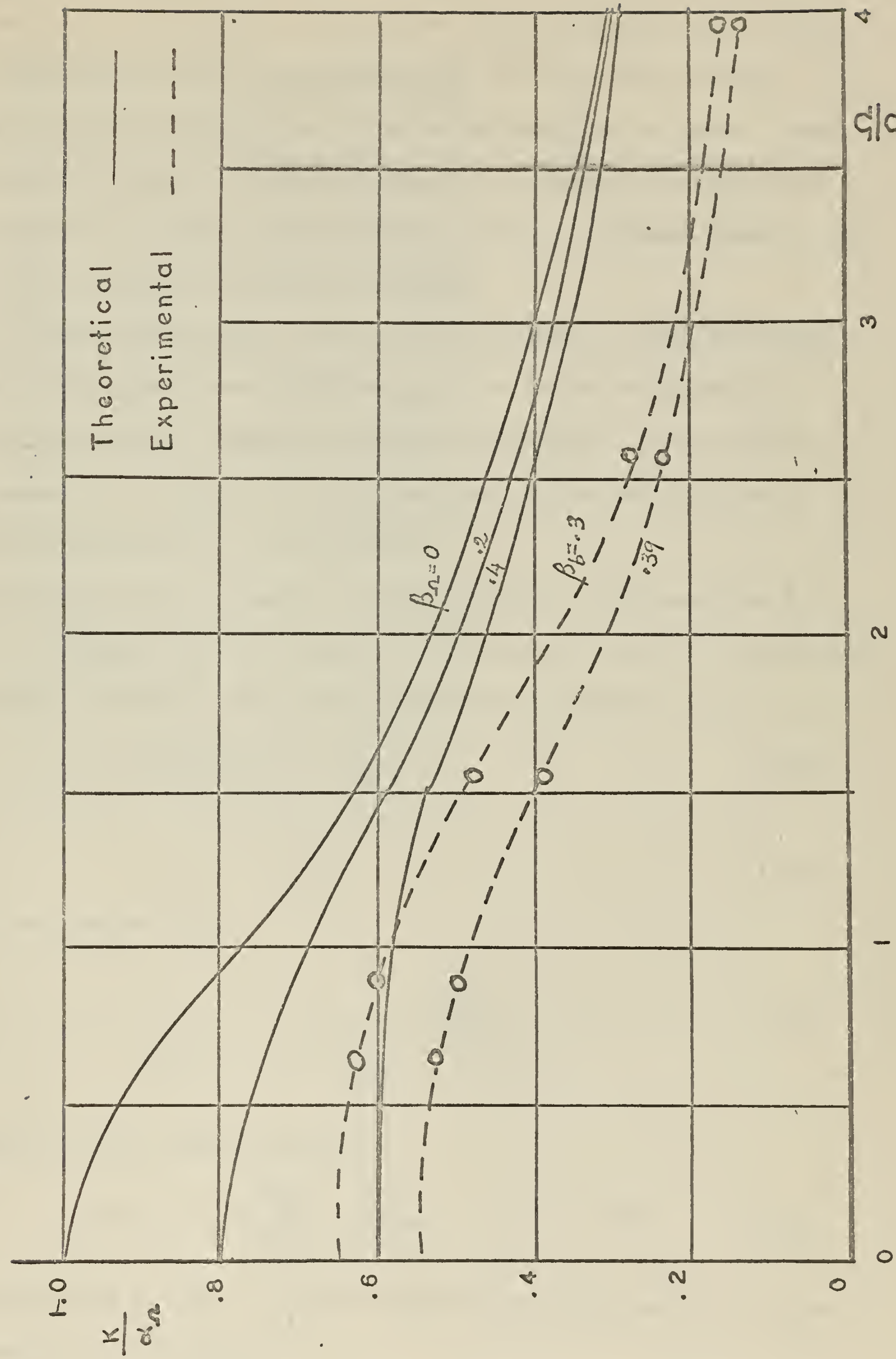

FIG. 14 - GAIN V/S SIGNAL FREQUENCY

Similarly for the case of the varying load resistance (Fig. 16). For a small load resistance, both equation (80) and experimental results show a linear relationship between the gain and the load resistance. If the load resistance is increased, this relationship is no longer linear, but there still exists an agreement between the theoretical and experimental results. If the load resistance is further increased beyond a certain limit, agreement is no longer expected.

It becomes evident that if the load resistance is increased beyond a certain limit, the first approximation is no longer sufficient and second or even higher approximation becomes necessary. It is, therefore, necessary to establish a limit for load resistance beyond which the first approximation is insufficient.

It is mentioned in Appendix B that if the first approximation ϕ_{yo} is to be sufficient and if the term in equations (32) and (33) monotonically decrease, the additional term ϕ_{y1} should be such that

$$|\rho_2|\,|\phi_{y1}| \ll |\phi_{yo}| \tag{143}$$

or

$$|\rho_2| \ll \left|\frac{\phi_{yo}}{\phi_{y1}}\right| \tag{144}$$

Since from equation (25)

$$|\rho_2| = \frac{R_2\left(1 + \frac{R_L}{2R_2}\right)\omega}{2\,N_2^2} \tag{145}$$

the inequality (144) may be written as

$$R_L \ll \left[\frac{|\phi_{yo}|}{|\phi_{y1}|}\;\frac{2N_2^2}{\omega R_2} - 1\right] 2\,R_2 \tag{146}$$

This establishes an upper limit for load resistance for which the first approximation is sufficient.

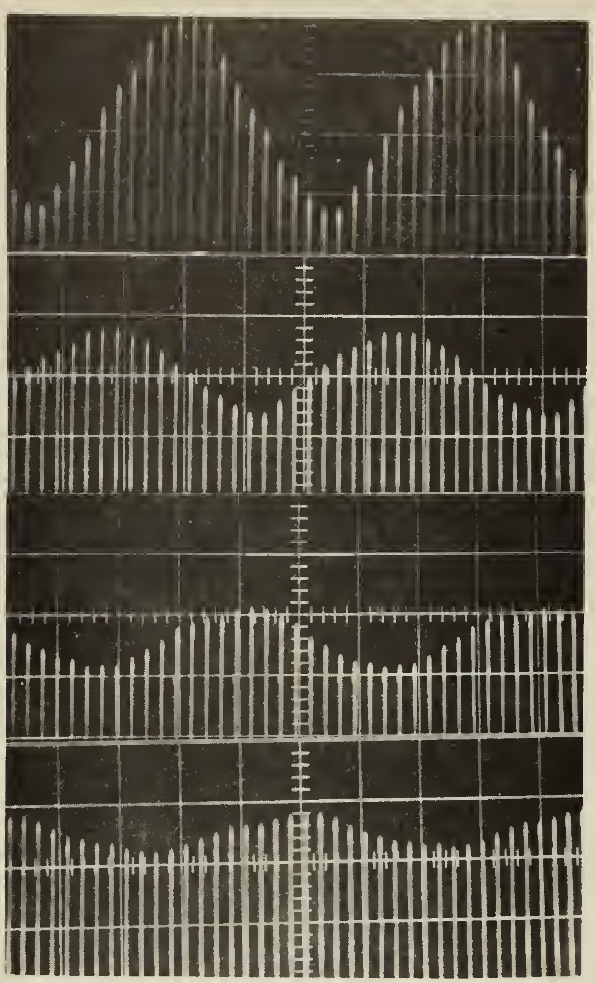

(a) $R_L = 0$

(b) $R_L = 5000$ ohms

(c) $R_L = 10\,000$ ohms

(d) $R_L = 15000$ ohms

FIG. 15 - ENVELOPES OF OUTPUT CURRENTS FOR DIFFERENT LOAD RESISTANCES

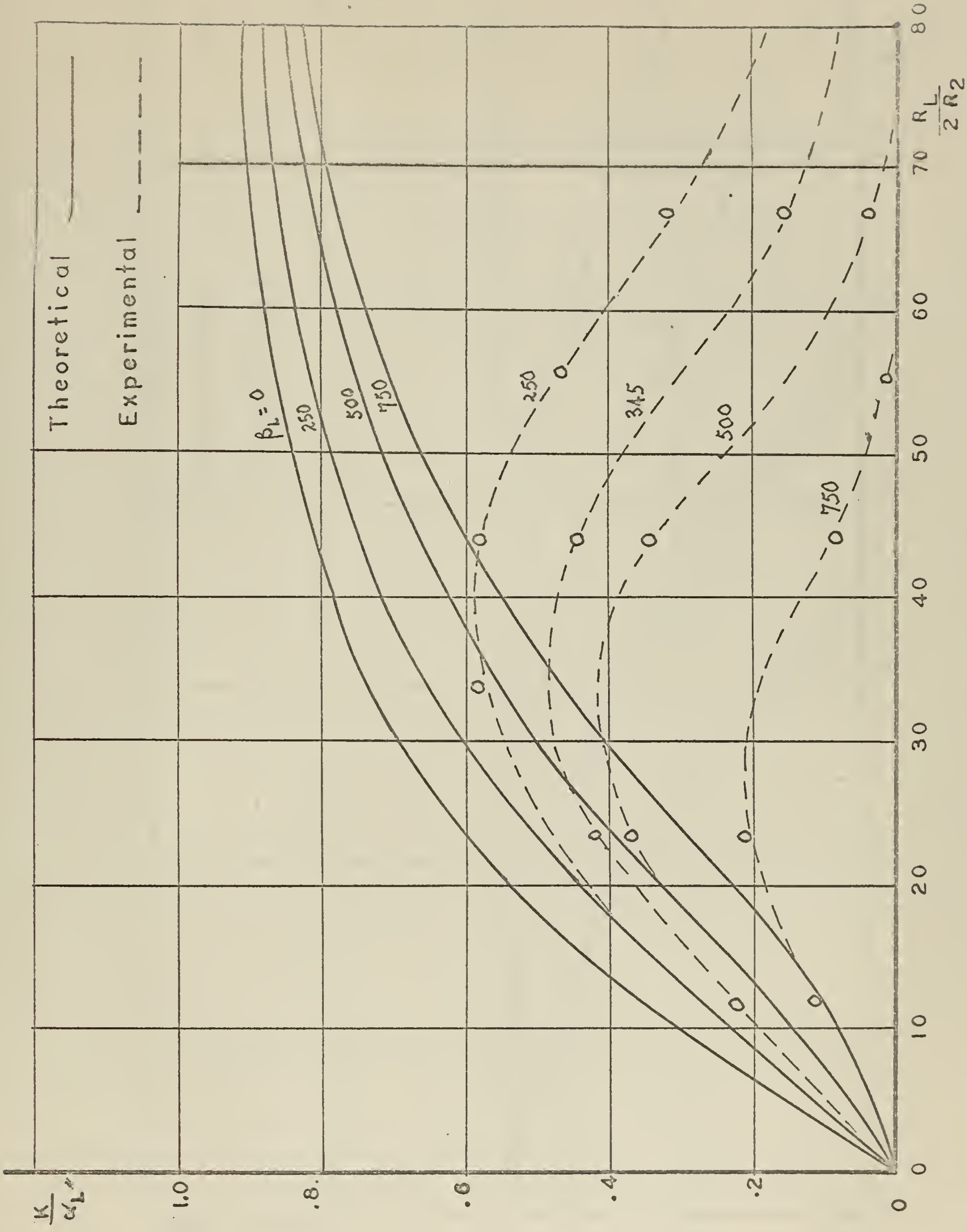

FIG. 16 - GAIN V/S LOAD RESISTANCE

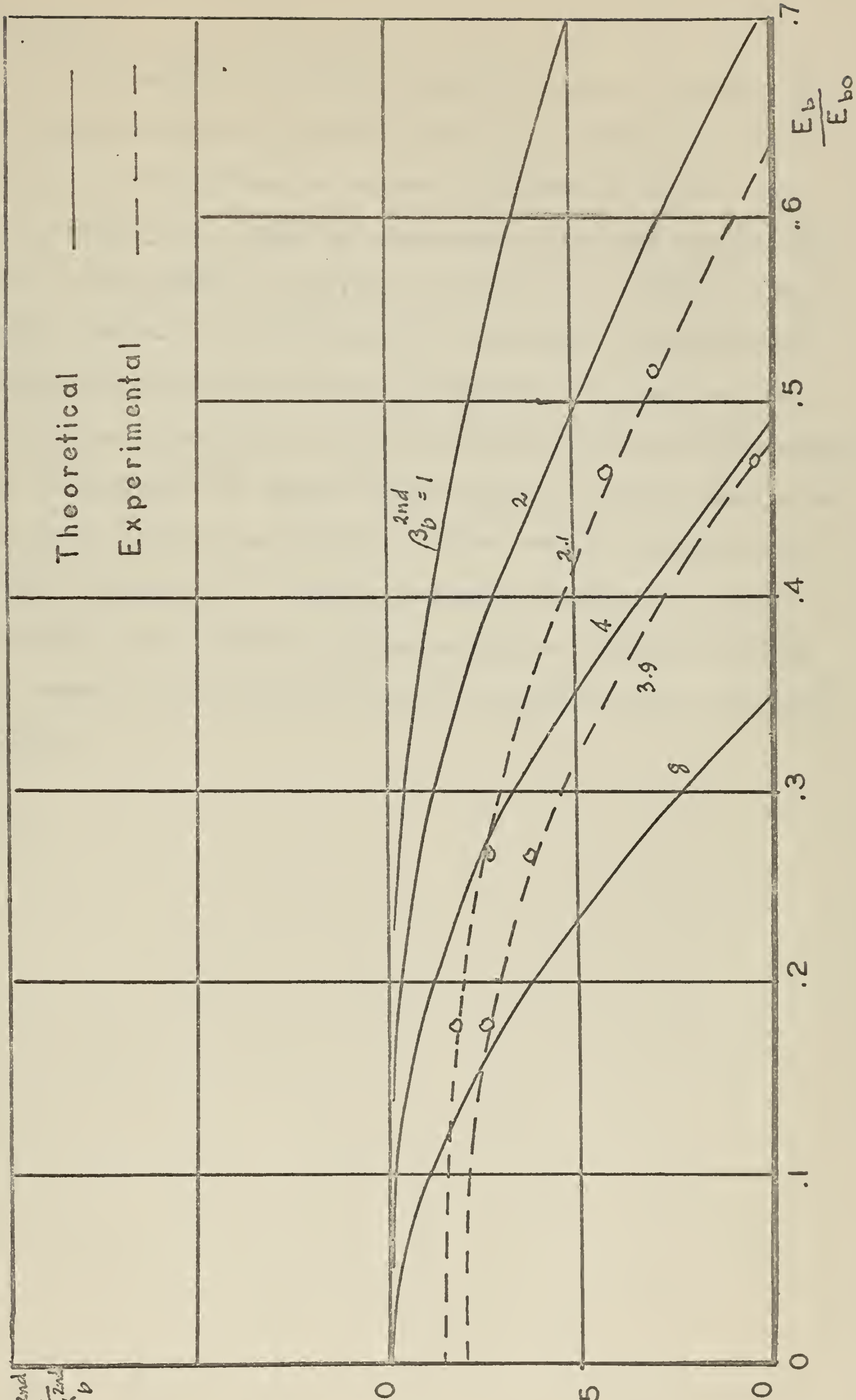

FIG. 17 – SECOND HARMONIC GENERATION PLOTTED AGAINST BIAS

IV-Conclusion -

The present analysis, principally concerned with the treatment of a series-connected magnetic amplifier including the effects of a resistive load, is mainly based on Poisson's perturbation method. The lack of knowledge of the region of convergence is the main disadvantage of the use of this method. This type of difficulty is inherent in most perturbation methods. In this particular application, the coefficient of nonlinear factor is usually small and negative. The smallness contributes to a rapid diminution of the contribution from successive approximations. In addition, its negative sign results in a series whose terms are alternately positive and negative. If the absolute values of the terms form a monotonic null sequence, the series converges. Furthermore, the error that results from approximating the infinite series by a finite number of terms does not exceed the absolute value of the first term omitted.

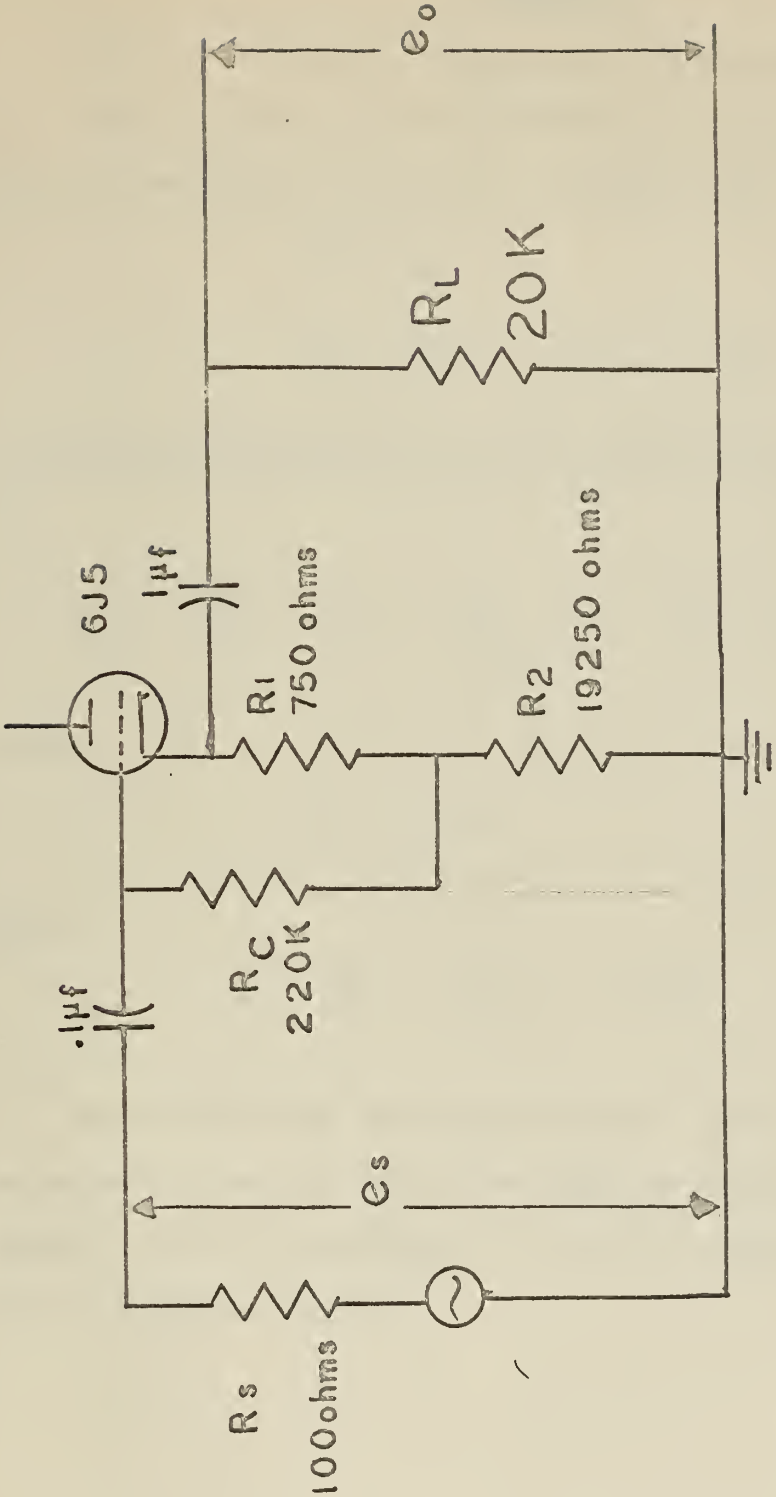

FIG.18 - CATHODE FOLLOWER

used in the input circuit of the experimental setup

APPENDIX A

Proof of convergence of Equations (30) and (31).

Since ϕ_x and ϕ_y are finite, there may be assigned a finite value $\phi_o/2$, by which both ϕ_x and ϕ_y are bounded, i.e.

$$\phi_x \leq \phi_o/2 \tag{147}$$

$$\phi_y \leq \phi_o/2 \quad \text{if} \quad \phi_x > \phi_y \tag{148}$$

Substituting (147) and (148) into equation (31), the latter is reduced to

$$i_2 \leq \frac{1}{N_2} \sum_{n}^{1,3,5\ldots} \left[k_n \left(\frac{\phi_o}{2} \right)^n \sum_{m}^{1,3,5\ldots n} \binom{n}{m} \right] \tag{149}$$

Since

$$\sum_{m} \binom{n}{m} = 2^n \tag{150}$$

then

$$i_2 \leq \frac{1}{N_2} \sum_{n}^{1,3,5\ldots} k_n \phi_o^n \tag{151}$$

Because the right hand side of equation (151) is a series known as convergent, therefore, the current response equations for i_2 is convergent too. The convergence of i_1 which is given by equation (30) can be proved the same way.

APPENDIX B

Sufficient conditions for the convergence of the Series given by equations (32) and (33)

The assumption that $\emptyset_x$ and $\emptyset_y$ may be represented by equations (32) and (33) is valid only if such series do converge. Otherwise, $\emptyset_x$ and $\emptyset_y$ cannot be represented by these equations and the present analysis is not applicable.

A sufficient condition for the convergence of these series can be established due to the fact that the small parameters ϵ_1 and ϵ_2 are negative. Thus, odd power term of equations (32) and (33) are of negative sign and even power term, of positive sign. There results a series whose terms are alternatively positive and negative. The sufficient condition for the convergence of such series according to Leibnitz theorem is that the absolute values of the terms form a monotonic null sequence, namely, for the present case,

$$|\epsilon_1| < \frac{|\emptyset_{x(n-1)}|}{|\emptyset_{x\,n}|} \tag{152}$$

and

$$|\epsilon_2| < \frac{|\emptyset_{y(n-1)}|}{|\emptyset_{y\,n}|} \tag{153}$$

Furthermore, the error that results from approximating the infinite series by a finite number of terms does not exceed the absolute value of the first term omitted.

APPENDIX C

Expressions of currents appearing in Equations (60) and (61)

$$I_{10} = \frac{k_1}{N_2} \phi_{2m} \left[1 + 3 \frac{k_3}{k_1} \left(\phi^2_{ob} + \frac{1}{2} + \phi^2_{1m} + \frac{1}{4} \phi^2_{2m} \right) \right. \tag{154}$$

$$\left. + 5 \frac{k_5}{k_1} \left(\phi^4_{ob} + \frac{3}{8} \phi^4_{1m} + \frac{1}{8} \phi^4_{2m} + 3 \phi^2_{ob} \phi^2_{1m} + \frac{3}{4} \phi^2_{1m} \phi^2_{2m} + \frac{3}{2} \phi^2_{2m} \phi^2_{ob} \right) \right]$$

$$I_{11} = 6 \frac{k_3}{N_2} \phi_{ob} \phi_{1m} \phi_{2m} \left[1 + \frac{10}{3} \frac{k_5}{k_3} \left(\phi^2_{ob} + \frac{3}{4} \phi^2_{1m} + \frac{3}{4} \phi^2_{2m} \right) \right] \tag{155}$$

$$I_{12} = - \frac{3}{2} \frac{k_3}{N_2} \phi^2_{1m} \phi_{2m} \left[1 + 10 \frac{k_5}{k_3} \left(\phi^2_{ob} + \frac{1}{6} \phi^2_{1m} + \frac{1}{4} \phi^2_{2m} \right) \right] \tag{156}$$

$$I_{13} = - 5 \frac{k_5}{N_2} \phi_{ob} \phi^3_{1m} \phi_{2m} \tag{157}$$

$$I_{14} = \frac{1}{8} \frac{k_5}{N_2} \phi^4_{1m} \phi_{2m} \tag{158}$$

$$I_{30} = - \frac{1}{4} \frac{k_3}{N_2} \phi^3_{2m} \left[1 + 10 \frac{k_5}{k_3} \left(\phi^2_{ob} + \frac{1}{2} \phi^2_{1m} + \frac{1}{8} \phi^2_{2m} \right) \right] \tag{159}$$

$$I_{31} = - 5 \frac{k_5}{N_2} \phi_{ob} \phi_{1m} \phi^3_{2m} \tag{160}$$

$$I_{32} = \frac{5}{4} \frac{k_5}{N_2} \phi^2_{1m} \phi^3_{2m} \tag{161}$$

$$I_{50} = \frac{1}{16} \frac{k_5}{N_2} \phi^5_{2m} \tag{162}$$

$$I_{00} = \frac{k_1}{N_1} \phi_{ob} \left[1 + \frac{k_3}{k_1} \left(\phi^2_{ob} + \frac{3}{2} \phi^2_{1m} + \frac{3}{2} \phi^2_{2m} \right) \right. \tag{163}$$

$$\left. + \frac{k_5}{k_1} \left(\phi^4_{ob} + \frac{15}{8} \phi^4_{1m} + \frac{15}{8} \phi^4_{2m} + 5 \phi^2_{ob} \phi^2_{1m} + \frac{15}{2} \phi^2_{1m} \phi^2_{2m} + 5 \phi^2_{2m} \phi^2_{ob} \right) \right]$$

$$I_{01} = \frac{k_1}{N_1} \phi_{1m} \left[1 + 3 \frac{k_3}{k_1} \left(\phi_{ob}^2 + \frac{1}{4} \phi_{1m}^2 + \frac{1}{2}\phi_{2m}^2 \right) \right. \tag{164}$$

$$\left. + 5\frac{k_5}{k_1} \left(\phi_{ob}^4 + \frac{1}{8} \phi_{1m}^4 + \frac{3}{8} \phi_{2m}^4 + \frac{3}{2} \phi_{ob}^2 \phi_{1m}^2 + \frac{3}{4} \phi_{1m}^2 \phi_{2m}^2 + 3\phi_{2m}^2 \phi_{ob}^2 \right) \right]$$

$$I_{02} = -\frac{3}{2} \frac{k_3}{N_1} \phi_{ob} \phi_{1m}^2 \left[1 + \frac{10}{3} \frac{k_5}{k_3} \left(\phi_{ob}^2 + \frac{1}{2}\phi_{1m}^2 + \frac{3}{2} \phi_{2m}^2 \right) \right] \tag{165}$$

$$I_{03} = -\frac{1}{4} \frac{k_3}{N_1} \phi_{1m}^3 \left[1 + 10 \frac{k_5}{k_3} \left(\phi_{ob}^2 + \frac{1}{8} \phi_{1m}^2 + \frac{1}{2} \phi_{2m}^2 \right) \right] \tag{166}$$

$$I_{04} = \frac{5}{8} \frac{k_5}{N_1} \phi_{ob} \phi_{1m}^4 \tag{167}$$

$$I_{05} = \frac{1}{16} \frac{k_5}{N_1} \phi_{1m}^5 \tag{168}$$

$$I_{20} = -\frac{3}{2} \frac{k_3}{N_1} \phi_{ob} \phi_{2m}^2 \left[1 + \frac{10}{3} \frac{k_5}{k_3} \left(\phi_{ob}^2 + \frac{3}{2} \phi_{1m}^2 + \frac{1}{2}\phi_{2m}^2 \right) \right] \tag{169}$$

$$I_{21} = -\frac{3}{2} \frac{k_3}{N_1} \phi_{1m} \phi_{2m}^2 \left[1 + 10 \frac{k_5}{k_3} \left(\phi_{ob}^2 + \frac{1}{4} \phi_{1m}^2 + \frac{1}{6} \phi_{2m}^2 \right) \right] \tag{170}$$

$$I_{22} = \frac{15}{2} \frac{k_5}{N_1} \phi_{ob} \phi_{1m}^2 \phi_{2m}^2 \tag{171}$$

$$I_{23} = \frac{5}{4} \frac{k_5}{N_1} \phi_{1m}^3 \phi_{2m}^2 \tag{172}$$

$$I_{40} = \frac{5}{8} \frac{k_5}{N_1} \phi_{ob} \phi_{2m}^4 \tag{173}$$

$$I_{41} = \frac{5}{8} \frac{k_5}{N_1} \phi_{1m} \phi_{2m}^4 \tag{174}$$

BIBLIOGRAPHY

1. Introduction to Nonlinear Mechanics by N. Minorsky, Edwards Brothers, Inc., 1947.

2. Advanced Calculus by I. S. Sokolnikoff, Theorem on Alternating Series, Page 234.

3. Mathematics of Modern Engineering by E. G. Keller, John Wiley and Sons, 1942.

4. Differential and Integral Calculus by R. Courant, Interscience Publishers, Inc., N. Y., 1949, Vol. 1.

5. The Fundamental Limitations of the Second Harmonic Type of Magnetic Modulator as Applied to the Amplification of Small D.C. Signal by F. C. Williams and S. W. Noble, Proc. of IEE, Vol. 8, Part III, 1951.

6. A Mathematical Analysis of Parallel-Connected Magnetic Amplifiers with Resistive Loads by L. A. Pipes, Journal of Applied Physics, Vol. 23, June 1952.

7. Comments on a Mathematical Analysis of Parallel-Connected Magnetic Amplifier with Resistive Loads by H. S. Kirschbaum, Journal of Applied Physics, February 1954.

8. Parallel-Connected Magnetic Amplifiers by S. H. Chow, Journal of Applied Physics, February 1954.

9. An Analysis of Transients in Magnetic Amplifiers by D. W. Ver Planck, L. A. Finzi and D. C. Beaumarriage, Trans. AIEE, Vol. 8, Part III, 1951.

10. Bibliography of Mangetic Amplifier devices and the Saturable Reactor Art, by James G. Miles, AIEE, Technical Paper, 51-388, September 1951.

11. Magnetic Amplifier by Storm, John Wiley Inc., 1955.